Accepted Manuscript

Design, synthesis, molecular modeling and anti-hyperglycemic evaluation of novel quinoxaline derivatives as potential PPARγ and SURs agonists

Mohamed.K. Ibrahim, Ibrahim H. Eissa, AbdallahE. Abdallah, Ahmed M. Metwaly, M.M. and M.A. Radwan ElSohly

PII: S0968-0896(16)31420-1
DOI: http://dx.doi.org/10.1016/j.bmc.2017.01.015
Reference: BMC 13494

To appear in: *Bioorganic & Medicinal Chemistry*

Received Date: 14 December 2016
Revised Date: 6 January 2017
Accepted Date: 11 January 2017

Please cite this article as: Ibrahim, Mohamed.K., Eissa, I.H., Abdallah, AbdallahE., Metwaly, A.M., Radwan ElSohly, M.M.a., Design, synthesis, molecular modeling and anti-hyperglycemic evaluation of novel quinoxaline derivatives as potential PPARγ and SURs agonists, *Bioorganic & Medicinal Chemistry* (2017), doi: http://dx.doi.org/10.1016/j.bmc.2017.01.015

Design, synthesis, molecular modeling and anti-hyperglycemic evaluation of novel quinoxaline derivatives as potential PPARγ and SURs agonists

Mohamed. K. Ibrahim [a], Ibrahim H. Eissa* [a], Abdallah E. Abdallah [a], Ahmed M. Metwaly[b], M. M. Radwan[c] and M. A. ElSohly*[c]

[a] Pharmaceutical Chemistry departments, Faculty of Pharmacy (Boys), Al-Azhar University, Cairo, 11884, Egypt

[b] Pharmacognosy department, Faculty of Pharmacy(Boys), University of Al-Azhar, Cairo, Egypt

[c] National Center for Natural Products Research, University of Mississippi, University, MS 38677, USA

* **Corresponding author:**

Ibrahim H. Eissa

Pharmaceutical Chemistry departments, Faculty of Pharmacy (Boys), Al-Azhar University, Cairo, 11884, Egypt

Email: Ibrahimeissa@azhar.edu.eg

M. A. ElSohly

National Center for Natural Products Research, University of Mississippi, University, MS 38677, USA

Email: Msohly@olemiss.edu

Abstract

In our effort to develop potent anti-hyperglycemic agents with potential agonistic activities toward PPARγ and SURs, three novel series of quinoxaline derivatives bearing sulfonylurea or sulfonylthiourea moieties with different linkers were designed and synthesized. Some of the newly synthesized compounds were evaluated *in vivo* for their anti-hyperglycemic activities in STZ-induced hyperglycemic rats. Compounds **15_a**, **15_e**, **19_b** and **24_a** exhibited the highest anti-hyperglycemic activities with % reduction in blood glucose level of (50.58, 43.84, 45.10 and 49.62, respectively). Additionally, eight compounds revealed potent anti-hyperglycemic activities were further evaluated *in vitro* for their PPARγ binding affinity and insulin-secreting ability as potential mechanisms for anti-hyperglycemic activity. Four compounds (**15_a**, **15_b**, **15_d** and **15_e**) significantly bound to PPARγ with IC_{50} values of 0.482, 0.491, 0.350 and 0.369 µM, respectively. Moreover, Compounds **15_a** and **15_b** have demonstrated induction of insulin-secretion with EC_{50} values of 0.92 and 0.98 µM, respectively. Furthermore, molecular docking and pharmacophore generation techniques were carried out to investigate binding patterns and fit values of the designed compounds with PPARγ and SUR, respectively.

Key words: Quinoxaline, PPARγ, Sulfonylurea, Sulfonylthiourea, Docking, Pharmacophore, Anti-hyperglycemic

1. Introduction

Type-2 diabetes mellitus (T2DM) is a disease often associated with a cluster of metabolic disturbances and cardiovascular risk factors such as obesity, insulin resistance, hypertension, atherosclerosis, dyslipidemia, and endothelial dysfunction [1]. So that, beyond glucose control, management of lipid metabolism have to be considered in the treatment of T2DM [2] .

The most important receptors involved in treatment of type II diabetes mellitus are peroxisome proliferator-activated receptors (PPARs) [3] and sulfonylurea receptors (SURs) [4] . PPARs are ligand activated transcription factors belonging to the nuclear hormone receptor super family. Three PPAR isotypes have been identified, PPAR α, δ and γ which are involved in the regulation of glucose and lipid homeostasis [5, 6]. PPARγ has an essential role in glucose metabolism and fatty acid storage, so that it is a crucial target for the development of insulin sensitizing anti-hyperglycemic agents [7].

The basic structural requirements for binding to PPARγ are an acidic head, a linker attached to an aromatic scaffold (spacer group), a linker, and a hetero-aromatic lipophilic tail [8, 9] (**Fig. 1A**). The most famous class of compounds reported as high-affinity PPARγ agonists are known as 'glitazones', or thiazolidinediones (TZDs), on the basis of their common 2,4 thiazolidinedione structural motif [10, 11]. A wide variety of lipophilic 'tails' have been reported to confer good anti-diabetic activity in TZDs and subsequently have been shown to bind and activate PPARγ [12]. The presence of a heterocyclic nitrogen atom in this region such as rosiglitazone **1**, pioglitasone **2**, darglitazone **3** [13], and imidazopyridine **4** [14] has been shown to confer excellent PPARγ potency. This nitrogen atom may serve as a hydrogen-bond acceptor to either a water molecule or a specific residue within this portion of the ligand binding domain (LBD)[15]. The lipophilic tail has usually been attached to the central 'spacer group' via an alkyl ether linkage [16]. The 2,4-thiazolidinedione 'head group' is usually linked to the 'spacer group' via a single methylene group. Shortening or lengthening of this linker , leads to a reduction of PPARγ agonistic activity [17]. Many groups have been reported on cyclic bioisosteric replacements of the 2, 4 thiazolidinedione head group as oxazolidinedione [18], oxadiazolidinedione [19] and isoxazolidine-3,5-diones [20]. Several acyclic TZD as N-hydroxyureas and carbonylated hydroxyureas have been reported as TZD replacements [19].

Unfortunately, the use of TZDs has been beset with adverse side effects such as congestive heart failure, myocardial infarction, weight gain and risk of death from cardiovascular causes [21, 22]. Therefore, demand for new PPARγ ligands other than TZD could be of special interest.

The second receptors are sulfonylurea receptors present in pancreatic β-cells. Sulfonylureas (SUs) stimulate insulin secretion via binding to sulfonylurea receptors [23]. The reported pharmacophoric features of sulfonylurea acting drugs are three lipophilic centers separated by an amide and an anionic linker (**Fig. 1B**). First generation sulfonylureas, such as tolbutamide, contain only two lipophilic centers and were proposed to interact with only A site of SURs. On the other hand, 2nd and 3rd generation sulfonylureas such as glipizide **7** and glimepiride **8** comprise amido (-CONH-) group which is required for interaction with B site of SURs [24]. Moreover, it was reported that some of 2nd and 3rd generation sulfonylureas exert their clinical efficacy by acting through both SURs and PPARγ [25-27]

1.1 Rationale of drug design

The great similarity between the basic structural requirements of PPARγ and SUR agonists drove us to design some novel compounds comprising both requirements (**Fig. 2**). The acidic head required to PPARγ agonistic activity, has been replaced by sulfonylurea or sulfonylthiourea moieties. Sulfonylurea and sulfonylthiourea moieties were incorporated into our molecules with the goal of providing PPARγ and SUR agonistic activities. They form hydrogen bonds with influencing residues of the protein active site (Ser289, His323, His449 and Tyr473) [28]. Aromatic and aliphatic substitutions on sulfonylurea and sulfonylthiourea moieties act as a lipophlic center required to SUR agonists. Moreover, NH group of sulfamoyl moiety is acidic (pKa = 4.9 – 6.5) and there for completely ionized at physiological pH [29]. This ionization produces an anionic linker which contributes significantly to SUR agonistic affinity [24]. Sulfonyl (SO_2) group acts as one atom spacer between an acidic head and aromatic group. This is considered as optimal length for PPARγ agonistic activity. Para-disubstituted phenyl group acts as an aromatic scaffold (spacer group) which is required for optimal PPARγ agonism [30], in addition to its role as lipophilic center for SUR agonists. Several linkers between lipophilic tail and an aromatic scaffold (spacer group) have been synthesized to study SAR of the new compounds. These linkers are essential for PPARγ agonistic activity, on the other hand, they contain amido(-CONH-) group which is required to interact with B site of SURs [24]. Finally, 3-methylquinoxalin-2(1H)-one and 3,4-dihydroquinoxalin-2(1H)-one nuclei, act as lipophilic tail and lipophlic center required for PPARγ and SURs agonistic activities, respectively.

The choice of quinoxaline nucleus was based on some bioisoeteric considerations. First, the bicyclic structure of quinoxaline core is convenient to the large size of the hydrophobic entrance of PPARγ active site [28]. Second, the heterocyclic nitrogen serves as a hydrogen-bond acceptor conferring excellent PPARγ potency.

Based on the above considerations, and in an attempt to obtain new multi-target antihyperglycemic agents, new scaffolds of quinoxaline-sulfonylurea hybrids have been designed and synthesized (**Fig. 2**).

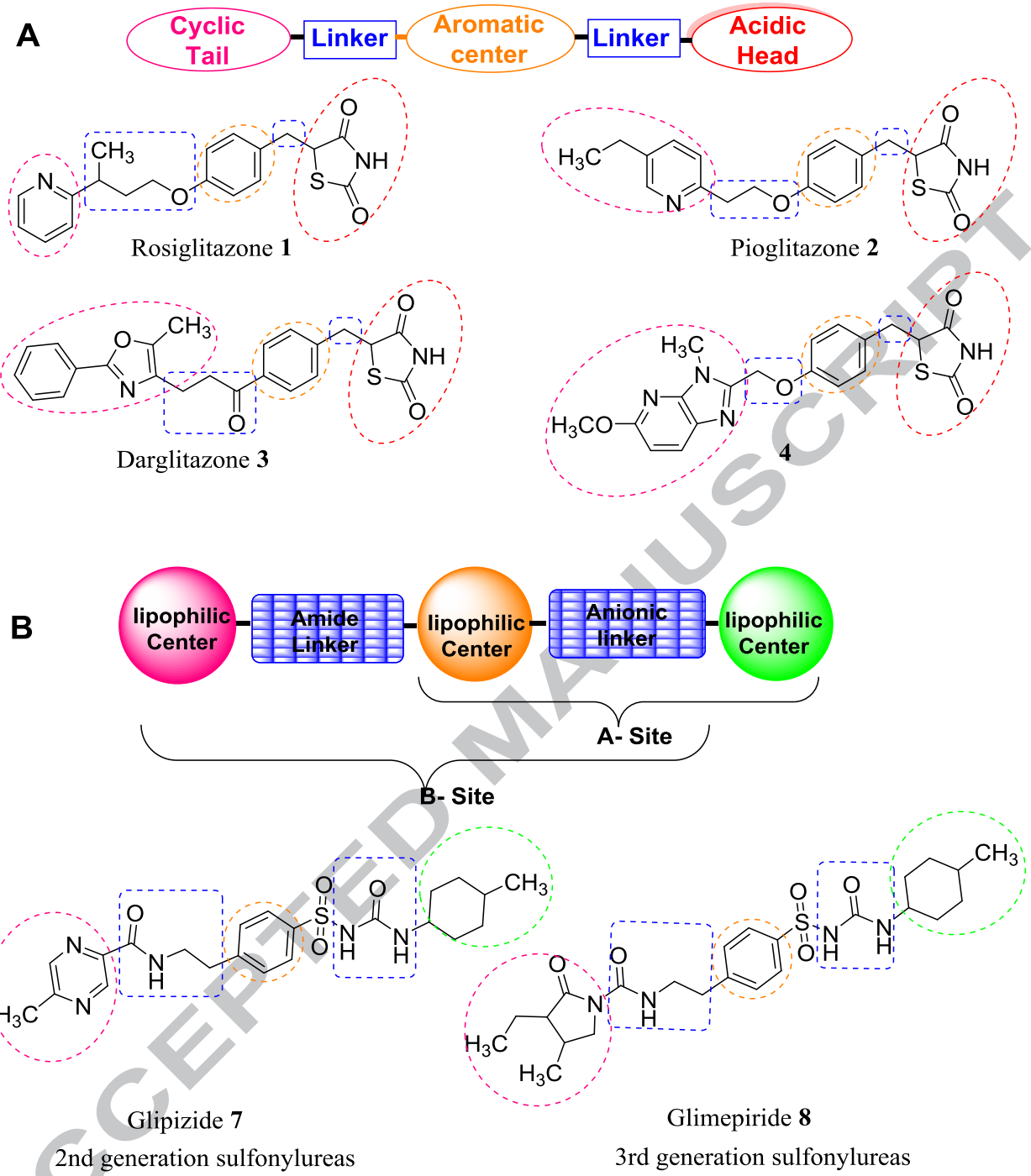

Fig. 1: (A): The basic structural features of PPARγ agonists and some reported compounds. **(B):** The basic structural features of sulfonylurea acting compounds and some reported compounds.

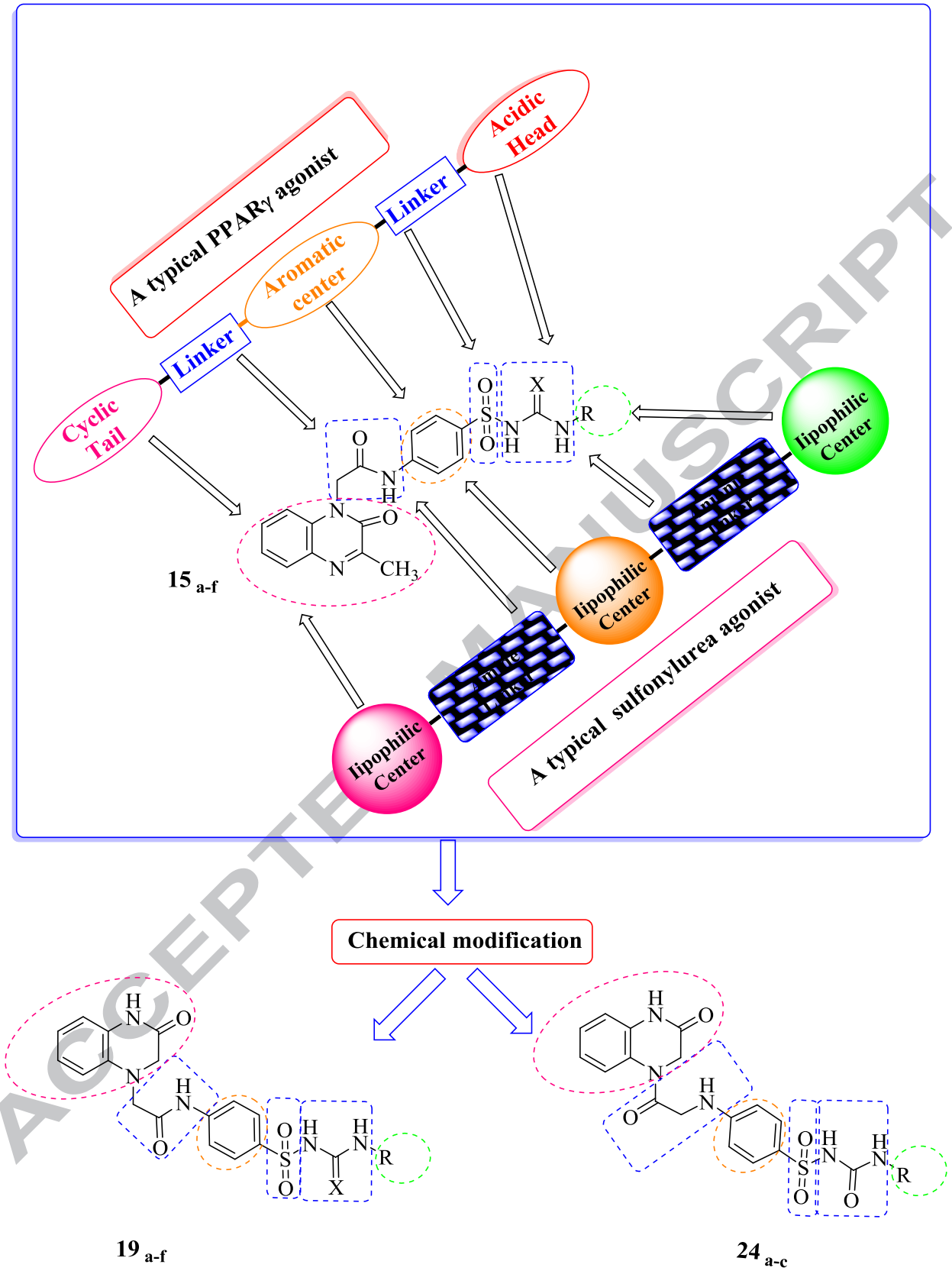

Fig. 2: Rationale of molecular design showing the basic structural requirements for PPARγ and SURs agonists.

2. Results and discussion

2.1. Chemistry

The sequence of reactions that was used in the synthesis of the target compounds is illustrated in **Schemes 1–3**. Synthesis was initiated by reaction of *o*-phenylenediamine **9** with sodium pyruvate **10** in glacial acetic acid to furnish 3-methylquinoxalin-2(1*H*)-one **11** [31], and subsequent treatment with alcoholic potassium hydroxide to afford the corresponding potassium salt **12** [32]. Heating of the obtained potassium salt with 2-chloro-*N*-(4-sulfamoylphenyl)acetamide **13** [33] in dry DMF afforded the key intermediate **14** in a good yield (76%). The reaction of compound **14** with the appropriate iso(thio)cyanates namely, cyclohexyl isocyanate, butyl isocyanate, phenyl isocyanate, cyclohexyl isothiocyanate, butyl isothiocyanate, and phenyl isothiocyanate in refluxing dry acetone in the presence of anhydrous potassium carbonate as a base afforded the target compounds **15$_{a-f}$**, respectively (**Scheme 1**).

Next, 3,4-dihydroquinoxalin-2(1*H*)-one **17** [34] was prepared via the reaction of *o*-phenylenediamine **9** with chloroacetic acid **16** in aqueous ammonia. Reaction of compound **17** with 2-chloro-*N*-(4-sulfamoylphenyl)acetamide **13** in dry DMF afforded the key intermediate **18** in a good yield (72.63%). Upon the reaction of compound **18** with the appropriate iso(thio)cyanates namely, cyclohexyl isocyanate, butyl isocyanate, phenyl isocyanate, cyclohexyl isothiocyanate, butyl isothiocyanate, and phenyl isothiocyanate in refluxing dry acetone with presence of anhydrous potassium carbonate as base, the target compounds **19$_{a-f}$** were produced (**Scheme 2**).

Finally, reaction of 3,4-dihydroquinoxalin-2(1*H*)-one **17** with chloroacetyl chloride in dry DMF afforded 4-(2-chloroacetyl)-3,4-dihydroquinoxalin-2(1*H*)-one **21** [35] and subsequent treatment with commercially available sulfanilamide afforded the intermediate compound **23.** The target compounds **24$_{a-c}$** were synthesized through the reaction of compound **23** with appropriate isocyanates namely, cyclohexyl isocyanate, butyl isocyanate and phenyl isocyanate, in refluxing dry acetone with presence of anhydrous potassium carbonate as a base. Structures of the target compounds were characterized by ^{1}H NMR, ^{13}C NMR, DEPT, IR and EI mass spectral data.

The IR spectra of the key compounds **14**, **18**, and **23** revealed the presence of two characteristic NH and NH_2 absorption bands of 4-aminobenzenesulfonamide moiety around 3382 - 3234 cm^{-1}, in addition to absorption bands due to C=O groups of quinoxaline and amide moieties around 1681-1657 cm^{-1}. Moreover, the two characteristic absorption bands of SO_2

group appeared around 1325 cm^{-1} and 1148 cm^{-1}. The IR spectra of compounds **15_{a-f}**, **19_{a-f}**, and **24_{a-c}** showed sharp absorption bands of 3NH groups of 4-aminobenzene sulfonyl(thio)urea moiety in the region 3383-3192 cm^{-1}.

The **^{1}H NMR** spectra of the key compounds **14**, **18**, and **23** revealed the presence of D_2O exchangeable singlet peak of sulfonamide NH_2 at about 7.2 ppm, and a singlet peak for the methylene group flanked between C=O and quinoxaline moieties at about 5.1 ppm. The **^{1}H NMR** spectra of compounds **15_{a-f}**, **19_{a-f}**, and **24_{a-c}** showed disappearance of sulfonamide NH_2 peak and appearance of more deshielded singlet peak for NH of sulfonylurea.

The aromatic area of compound **14** showed a characteristic *para*-disubstituted benzene ring pattern at 7.51 (d, *J* = 6.0 Hz, 2H) and 7.73 (d, *J* = 6.0 Hz, 2H).

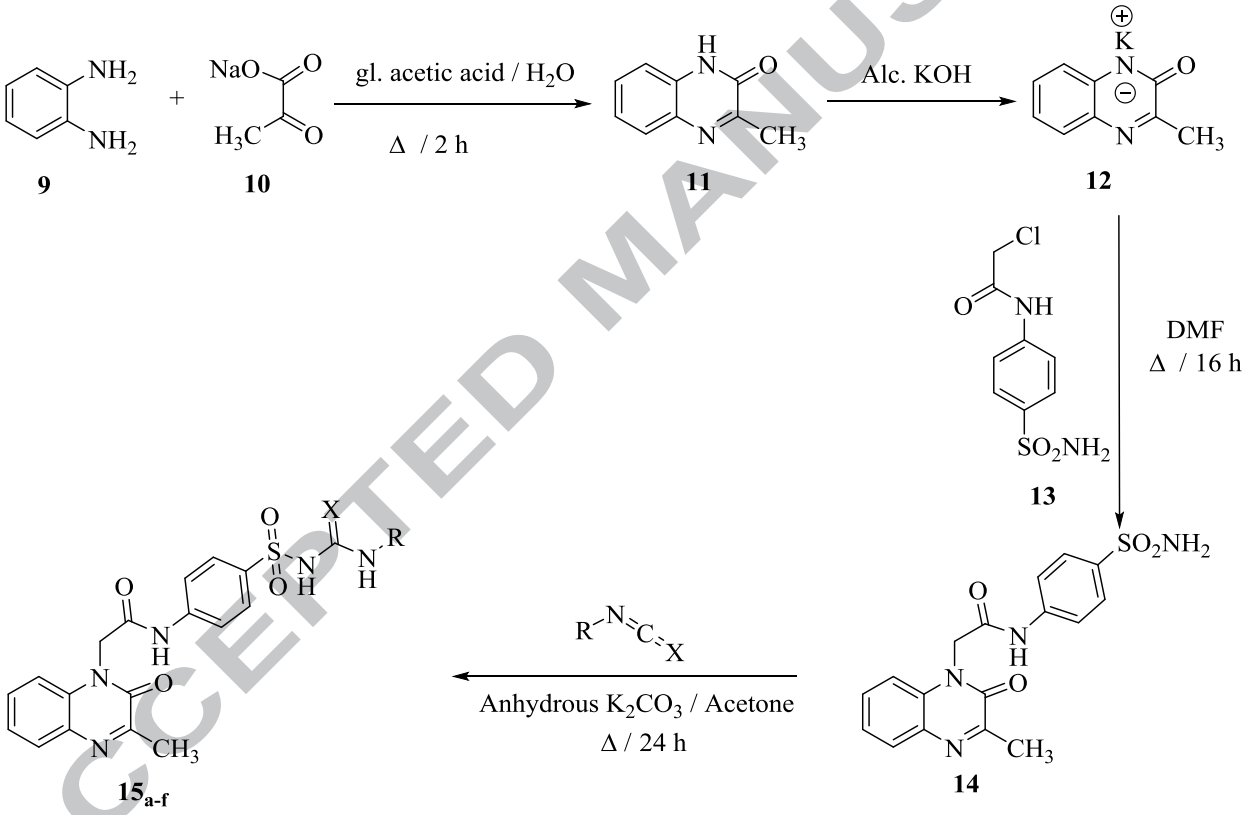

a) R= Cyclohexyl, X = O
b) R= Butyl , X = O
c) R= Phenyl, X = O
d) R= Cyclohexyl, X = S
e) R= Butyl , X = S
f) R= Phenyl, X = S

Scheme 1: General procedure for preparation of target compounds **15_{a-f}**

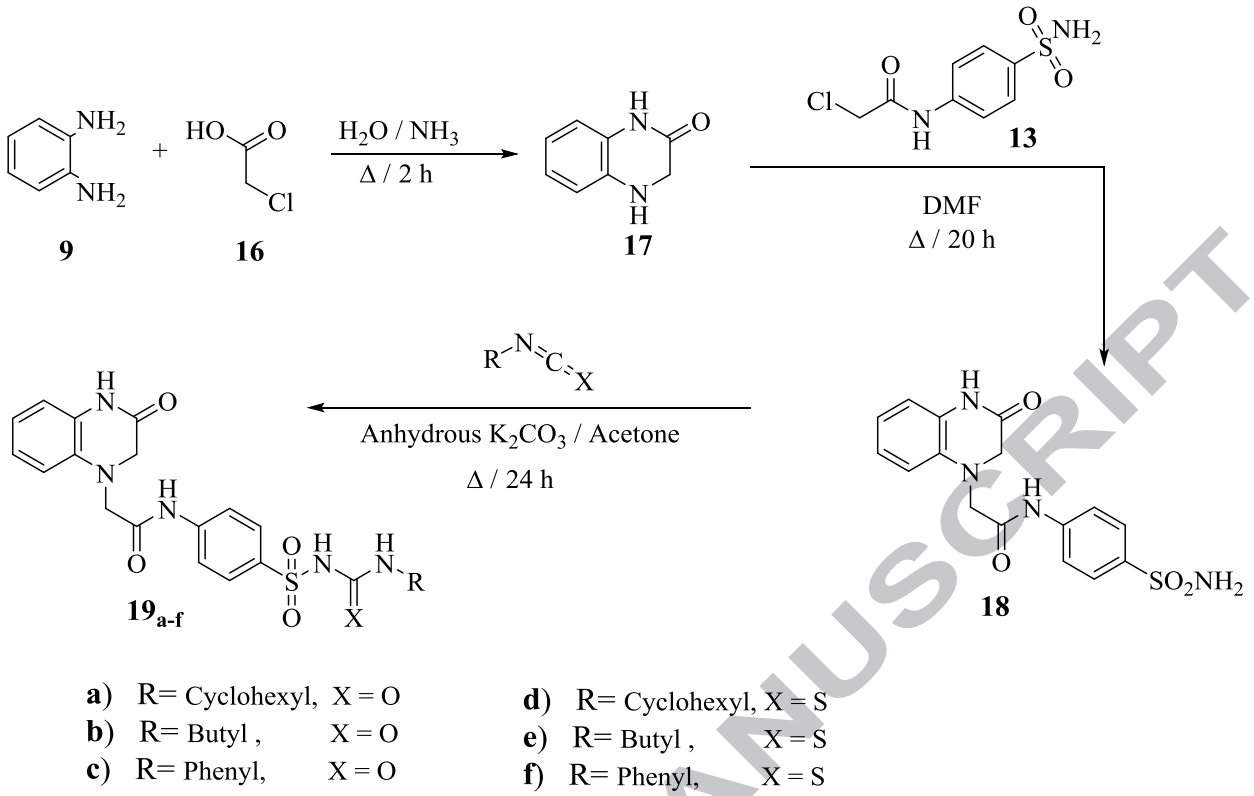

a) R= Cyclohexyl, X = O
b) R= Butyl , X = O
c) R= Phenyl, X = O
d) R= Cyclohexyl, X = S
e) R= Butyl , X = S
f) R= Phenyl, X = S

Scheme 2: General procedure for preparation of target compounds $\mathbf{19_{a-f}}$

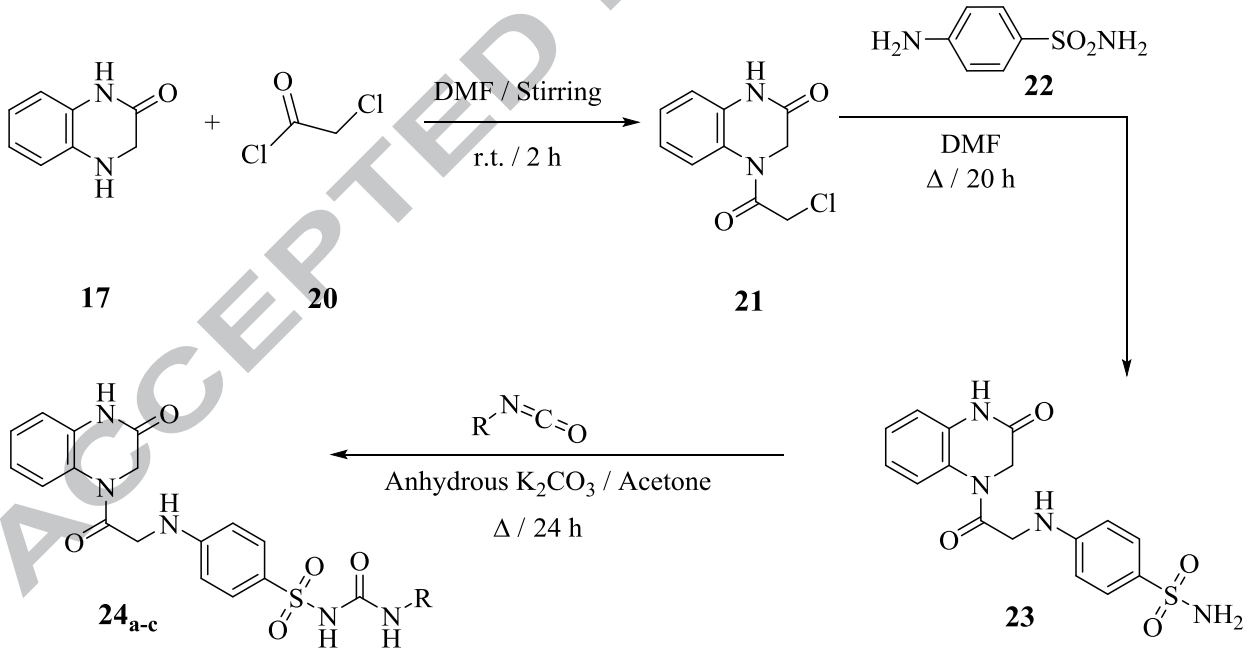

a) R= Cyclohexyl, **b)** R= Butyl **c)** R= Phenyl

Scheme 3: General procedure for preparation of target compounds $\mathbf{24_{a-c}}$

2.2. Biological testing

2.2.1. *In vivo* anti-hyperglycemic activity

The *in vivo* anti-hyperglycemic activity of the newly prepared compounds **15_{a-f}**, **19_{a-f}** and **24_{a-c}** was examined against streptozotocin-induced hyperglycemic rats using anti-hyperglycemic assay as described by Ramsey *et al* [36]. Rosiglitazone and glimepiride were included in the experiment as positive controls. The results were expressed as % reduction in blood glucose level (**Table 1**). Most of the synthesized compounds showed excellent to modest anti-hyperglycemic activity against streptozotocin-induced hyperglycemic rats. Compound **15_a** was found to be the most potent derivatives (% reduction in blood glucose level of50.58). Besides, compounds **24_a**, **19_b** and **15_e** possessed strong anti-hyperglycemic activities (% reduction in blood glucose level of 49.62, and 45.10, 43.84, respectively). Several compounds showed good anti-hyperglycemic activity as **15_b**, **24_b** and **19_a** (% reduction in blood glucose level of 40.55, 40.55 and 39.81, respectively). Moreover, compounds **15_c**, **15_d**, **15_f**, **19_c**, **24_c** and **19_e** were moderately active with % reduction in blood glucose level values ranging from 33.23 to 20.54. On the other hand, Compounds **19_d** and **19_f** were found to the weakest anti-hyperglycemic agents (% reduction in blood glucose level of 13.08, and 2.88, respectively).

2.2.2. *In vitro* PPARγ- ligand binding assay

Compounds with strong in *vivo* anti-hyperglycemic activities (**15_a**, **15_b**, **15_d**, **15_e**, **19_a**, **19_b**, **24_a**, and **24_b**) were further evaluated to determine their *in vitro* binding affinity to PPARγ. The ability of these compounds to bind with the PPARγ-LBD have been assessed through Fluorescence Polarization Assay technique [37]. Rosiglitazone was used as a positive control. **Table 1** shows a comparison of IC_{50} values for the test compounds. Compounds **15_a**, **15_b**, **15_d** and **15_e** significantly bound to PPARγ with IC_{50} values of 0.482, 0.491, 0.350 and 0.369 µM, respectively. The results were not significant as rosiglitazone. Rosiglitazone PPARγ binding affinity was 1.6, 1.7, 1.2 and 1.3 folds stronger than **15_a**, **15_b**, **15_d** and **15_e**, respectively. On the other hand, compounds **19_a**, **19_b**, **24_a** and **24_b** showed moderate PPARγ binding affinities with IC_{50} values ranging from 1.141 to 1.320 µM.

2.2.3. *In vitro* insulin assay

Compounds (**15_a**, **15_b**, **15_d**, **15_e**, **19_a**, **19_b**, **24_a**, and **24_b)** were further evaluated to determine their *in vitro* insulin-secreting activities against isolated pancreatic islets of rats via quantitative sandwich enzyme immunoassay technique [38]. Glimiperide was used as a positive control. The results were reported as the EC_{50} values (**Table 1**).

The examined compounds exhibited good to moderate insulin-secreting activities with EC_{50} values ranging from 0.92 to 2.82 µM. Glimiperide showed EC_{50} of 0.73 µM. Compounds **15_a** and **15_b** have demonstrated potent insulin-secreting activities with EC_{50} values of 0.92 and 0.98 µM, respectively. Compounds **19_a**, **19_b**, **24_a**, and **24_b** exhibited moderate activities with IC_{50} values of 1.54, 1.69, 1.89 and 1.95 µM, respectively. Moreover, compounds **15_d** and **15_e** displayed weak insulin-secreting activities with IC_{50} values of 2.69 and 2.82 µM, respectively.

Table 1: *In vivo* reduction in blood glucose levels, *in vitro* PPARγ binding affinities and *in vitro* insulin secreting activities of the newly synthesized compounds and reference drugs

Comp.	*In vivo*[a]	*in vitro*[a]	
	Reduction in blood glucose level (%)	PPARγ binding affinity IC_{50} (μM)[b]	Insulin Secreting activity EC_{50} (μM)[c]
15$_a$	50.58	0.482	0.92
15$_b$	40.55	0.491	0.98
15$_c$	25.15	NT[d]	NT[d]
15$_d$	33.23	0.350	2.69
15$_e$	43.84	0.369	2.82
15$_f$	20.54	NT[d]	NT[d]
19$_a$	39.81	1.150	1.54
19$_b$	45.10	1.293	1.69
19$_c$	21.89	NT[d]	NT[d]
19$_d$	13.08	NT[d]	NT[d]
19$_e$	30.75	NT[d]	NT[d]
19$_f$	2.88	NT[d]	NT[d]
24$_a$	49.62	1.141	1.89
24$_b$	40.55	1.320	1.95
24$_c$	22.01	NT[d]	NT[d]

Rosiglitazone	32.21	0.292	NT[d]
Glimiperide	26.53	NT[d]	0.73

[a] All data within 10 % (n = 3)

[b] Concentration of the test compound required to displace 50% of titrated ligand

[c] Concentration required to produce 50% of maximal effect.

[d] NT: Compounds not tested

2.3. Molecular modeling

Many crystal structures of PPARγ receptor are available in the Protein Data Bank (PDB). So that, receptor based drug design (docking) technique [39] was selected to investigate the binding pattern of the synthesized compounds with the prospective target, PPARγ. Since the crystal structure for SUR is not available, ligand based drug design (pharmacophore) technique [40] was used as a guide to predict the sulfonylurea agonistic activities of the synthesized compounds to give an idea on the interaction that would exist between the ligand and the receptor.

2.3.1. Docking studies

To predict the PPARγ agonistic activity of the synthesized compounds, docking studies were carried out using Discovery studio software program [41]. The PPARγ cavity is Y-shaped and consists of an entrance, arm I and arm II. Arm I contains four polar residues, Ser289, His323, His449 and Tyr473. These residues involved in hydrogen bond network between the receptor and ligands. Arm II is formed from Ile 341, Leu353, Ile281 and Val339 while the entrance consists of Leu330, Leu333, Ser342 and Arg288 [28] (**Fig.3**).

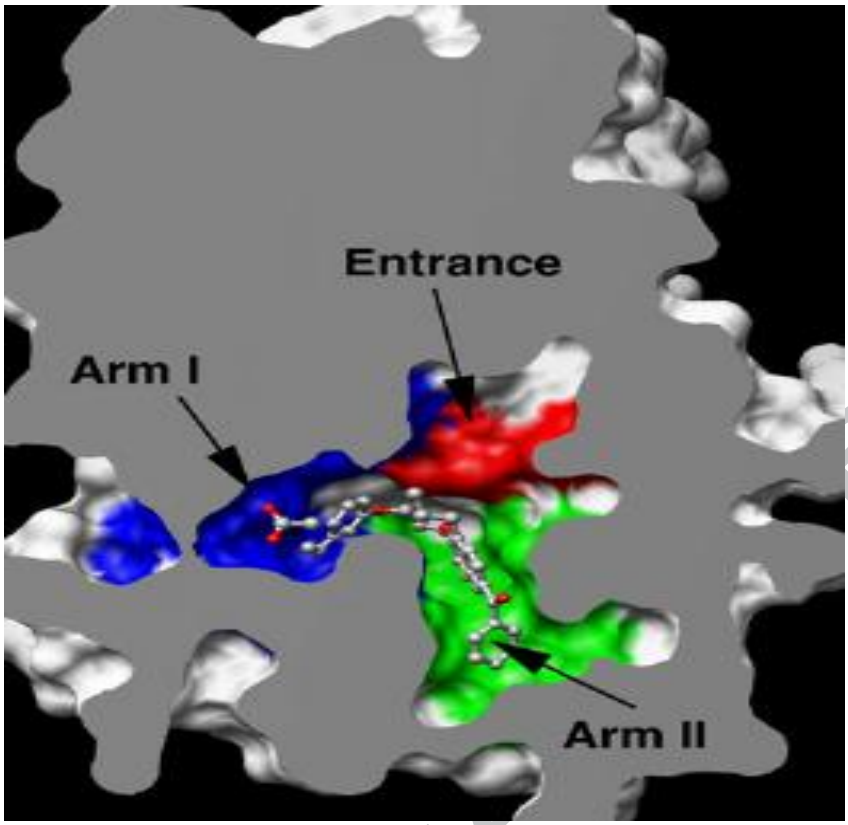

Fig. 3: PPARγ cavity composed of 3 main parts arm I, arm II and entrance [28]

The proposed binding mode of the ligand, rosiglitazone, revealed an affinity value of -48.74 kcal/mol. It demonstrated the important interactions with the residues at the active site of PPARγ. The acidic polar thiazolidinedione head is oriented in the polar arm I of the receptor where the acidic hydrogen of the imide group formed a hydrogen bond with a distance of 2.38 A˚ with Tyr473 (OH). The hydrophobic tail occupied the hydrophobic pocket (arm II and the hydrophobic part of the entrance),These results were found to be identical with the reported data [28] (**Fig. 4**).

The obtained results indicated that all studied ligands showed a similar position and orientation inside the putative binding site of PPARγ. All designed molecules exhibited good binding energies ranging from – 36.62 to -55.52 kcal/mol (**Table 2**). The proposed binding mode of compound **15_e** (affinity value of -50.81 kcal/mol with four hydrogen bonds) was virtually the same like that of rosiglitazone (**Fig. 5**). The acidic polar head (sulfonylthiourea moiety) was oriented in the polar arm I and formed two hydrogen bonds with the polar residues Tyr327 and His449. The acidic hydrogen of the sulfamoyl group formed a hydrogen bond with a distance of 2.07 A˚ with Tyr327 (OH) and the carbamothioyl group formed a hydrogen bond with a distance

of 2.02 A˚ with His449 (nitrogen of imidazole ring). The heterocyclic quinoxaline moiety was oriented in the hydrophobic entrance. The nitrogen heteroatom of quinoxaline moiety formed a hydrogen bond and a cationic pi bond with a distance of 2.39 and 4.90 A˚ with Ser342 (HN) and Arg288, residues of entrance, respectively.

The proposed binding mode of compound **15_b** (affinity value of -55.52 kcal/mol with two hydrogen bonds) was virtually the same as that of rosiglitazone, where its acidic polar head (sulfonylurea moiety) occupied the polar arm I. It formed two hydrogen bonds; the sulfamoyl group formed a hydrogen bond via its acidic hydrogen with a distance of 2.43 A˚ with Tyr473 (OH). The carbamoyl group formed a hydrogen bond with a distance of 2.47 A˚ with His323 (nitrogen 2 of imidazole ring) (**Fig. 6**).

Table 2: The docking binding free energies of the synthesized compounds

Comp. No.	Binding free energy (kcal/mol)	Comp. No	Binding free energy (kcal/mol)
15_a	- 46.31	**19_c**	- 46.52
15_b	- 55.52	**19_d**	- 45.31
15_c	- 47.33	**19_e**	- 46.73
15_d	- 36.62	**19_f**	- 53.43
15_e	- 50.81	**24_a**	- 52.91
15_f	- 40.23	**24_b**	- 50.44
19_a	- 52.43	**24_c**	- 47.92
19_b	- 52.23	**Rosiglitazone**	- 48.74

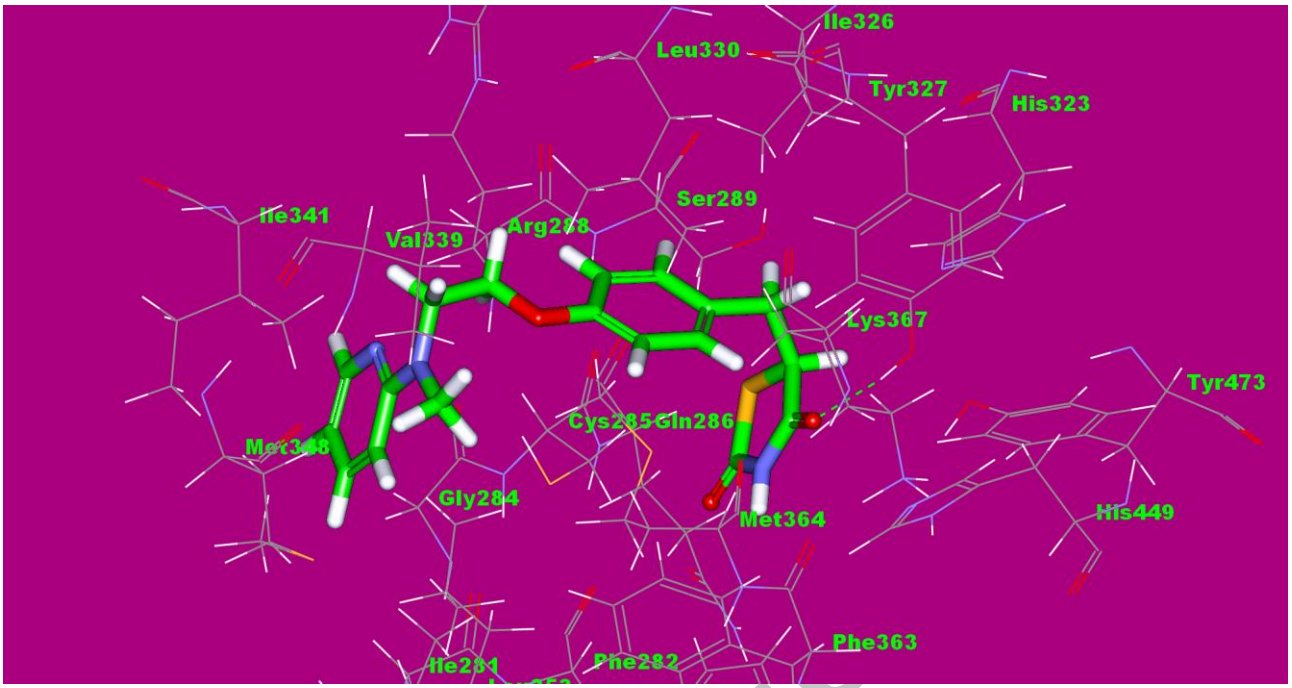

Fig. 4: Rosiglitazone docked into the active site forming hydrogen bond (green dot) between its polar head and tyr473

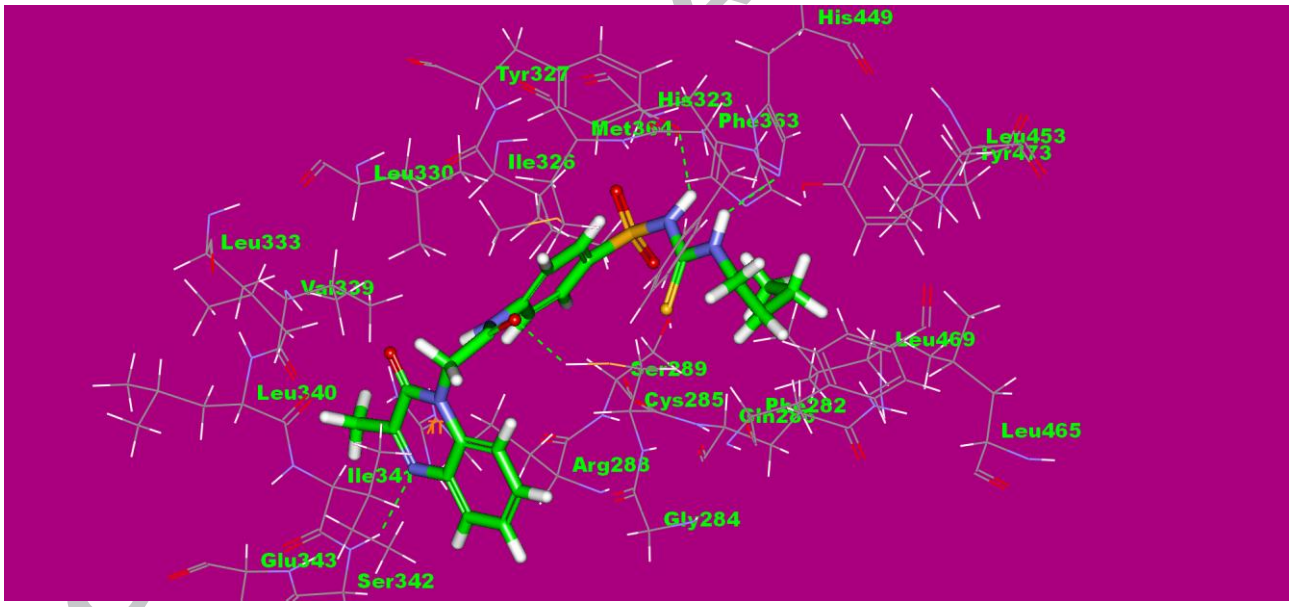

Fig. 5: Compound **15$_e$** docked into the active site, and its polar head formed hydrogen bonds (green) with the polar residues (Tyr327 & His449) in arm I. Quinoxaline moiety formed hydrogen bond with Ser342 residue of entrance.

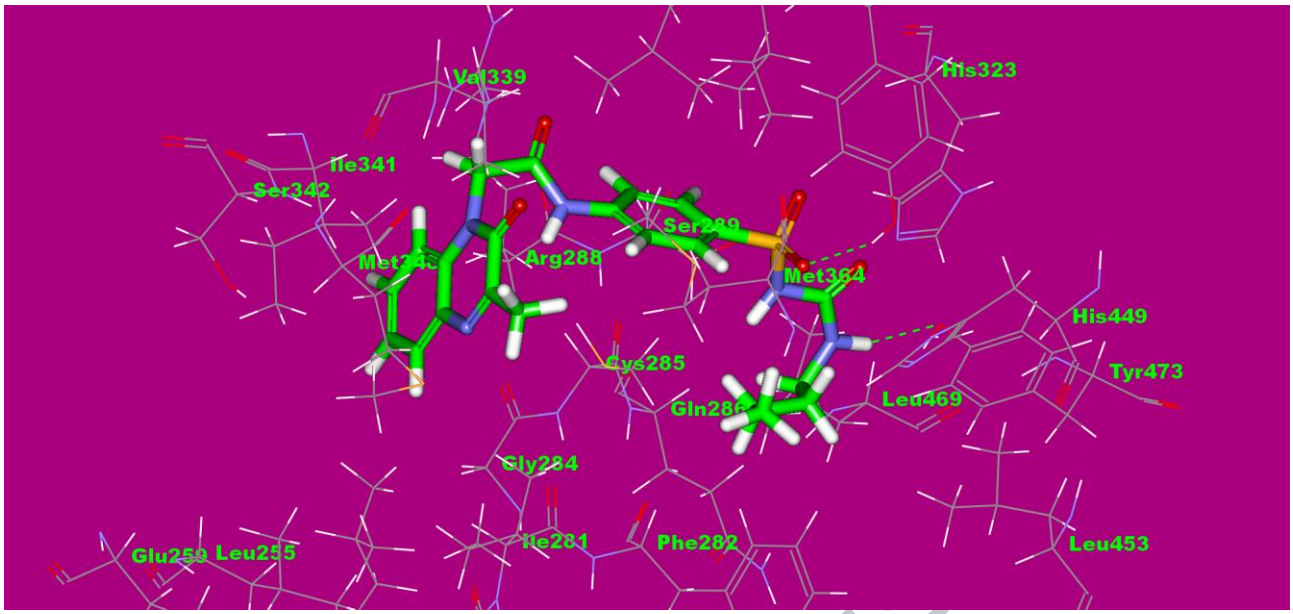

Fig. 6: Compound **15$_b$** docked into the active site, and its polar head formed hydrogen bonds (green) with the influencing polar residues Tyr473 and His323 in arm I

2.3.2. Pharmacophore study

2.3.2.1. Generation of 3D-pharmacophore model

The main objective of this technique was to generate 3D pharmacophore models based on the known SU agonists, which can correctly reflect the SAR of the existing SU agonists. Then, this generated model was used as 3D search query for evaluating the synthesized compounds and identify SU agonistic activities. Ten hypotheses were generated (**Table 3**). All of them have cost difference more than 60 bits and correlation coefficient values higher than 0.87. Cost difference is the difference between the total cost of the null hypothesis and total cost of the generated hypothesis. In general if the cost difference higher than 60 bits, there is an excellent chance (more than 90 %) the model represents a true correlation. Hypo 1 total cost is the closet to the fixed cost, RMS is the smallest and the correlation coefficient is the highest so that it was selected as the best hypothesis and employed for further analyses. The null cost, fixed cost and hypo 1 total cost values are 141.54, 48.60 and 68.09 bits respectively. Hypo 1 cost difference is 73.45, RMS is 1.88 and correlation coefficient is 0.91. All hypotheses except the tenth one comprised the following features; two hydrogen bond acceptors (HBA) (some of them comprised one hydrogen bond acceptor (HBA) and hydrogen bond acceptor (HBF)), hydrophobic aliphatic (HA) and ring aromatic (RA) (**Table 3**).

Table 3. Information of statistical significance and predictive power of top 10 hypotheses as a result of applying of HypoGen pharmacophore generation to the training set.

Hypo no.	Total cost	Cost difference [a]	RMS[b]	Correlation	Features[c]	Max. fit
Hypo 1	68.09	73.45	1.88	0.91	HBA, HBA, HA, RA	8.36
Hypo 2	68.67	72.87	1.91	0.91	HBA, HBA, HA, RA	7.74
Hypo 3	70.64	70.90	1.99	0.90	HBA, HBA, HBA, HA	8.43
Hypo 4	72.84	68.70	2.10	0.89	HBA, HBA, HBD, HA	8.34
Hypo 5	73.66	67.88	2.13	0.89	HBA, HBA, HA, RA	7.31
Hypo 6	74.19	67.35	2.16	0.88	HBA, HBD, HA, RA	8.78
Hypo 7	74.28	67.26	2.13	0.89	HBA, HBA, HBD, HA	6.65
Hypo 8	74.42	67.12	2.17	0.88	HBA, HBA, HBA, HA	8.17
Hypo 9	74.43	67.11	2.17	0.88	HBA, HBA, HA, RA	8.03
Hypo 10	74.78	66.76	2.16	0.88	HBD, HA, RA	5.06

[a] Cost difference is the difference between null cost and total cost. Null cost = 141.54, fixed cost = 48.60, configuration cost = 21.44, cost unit is bit.

[b] RMS, root mean square deviation, the deviation of log estimated activities from log experimental activities normalized by log uncertainty.

[c] Abbreviation used for features: HBA, hydrogen bond acceptor; HBD, hydrogen bond donor; HA, hydrophobic aliphatic; RA, ring aromatic.

Hypo 1 consists of hydrophobic aliphatic (HA), ring aromatic (RA) and two hydrogen bond acceptors (HBA) (**Fig. 7**). The spatial arrangement and the distances between the pharmacophore features of hypo 1 are demonstrated in **Fig. 8**. The results of this study confirmed the reliability of the generated pharmacophore model.

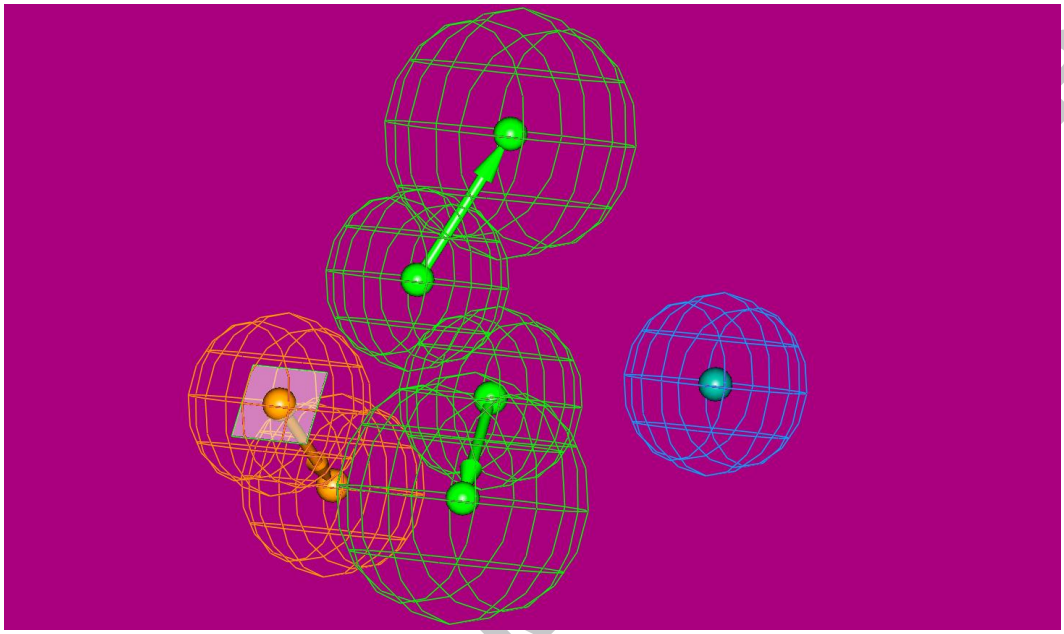

Fig. 7: The best hypothetical 3D-pharmacophore geometry (Hypo 1) with four features; two H-bond acceptors (green color), hydrophobic aliphatic (blue), aromatic ring (brown).

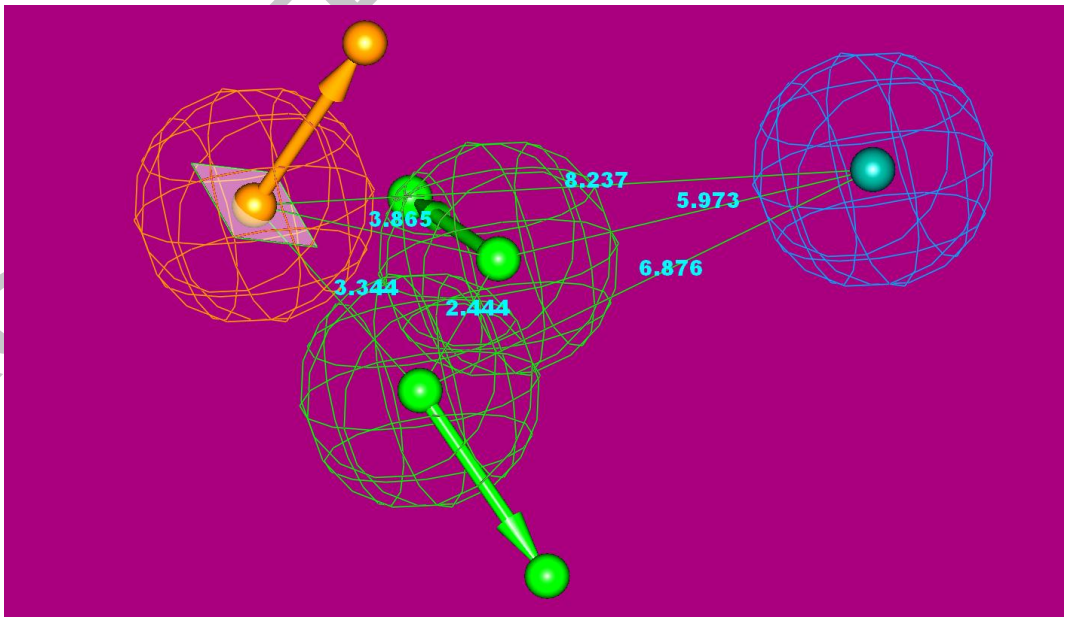

Fig. 8: 3D spatial relationship and geometric parameters of Hypo1. The distance between Pharmacophore features is reported in angstroms.

The Hypo1 predictability was internally evaluated by using compounds of training set divided on the basis of their activity scale in to; highly active (+++, 1/C < 10 μM), moderately active (++, 10 μM ≤ 1/C < 100 μM) and inactive (+, 1/C ≥ 100 μM). The validation results indicated that there is no inconsistency between experimental and predicted activity values for all compounds. **Table 4** shows the experimental and estimated 1/C values of training set molecules with error values, fit values and matching degrees with the pharmacophore Hypo-1.

Table 4. Experimental and estimated activities of the training set compounds based on pharmacophore model hypo 1.

Comp.	Exp.[a] (μM)	Est[b] (μM)	Exp. scale[c]	Est. scale[c]	Fit value[d]	Error[e]
25$_a$	1.60	2.36	+++	+++	7.77	1.47
25$_b$	12.50	11.40	++	++	7.09	-1.10
25$_c$	3.40	2.34	+++	+++	7.78	-1.46
25$_d$	3.10	2.34	+++	+++	7.78	-1.32
25$_e$	2.40	2.81	+++	+++	7.70	1.17
26$_a$	33.30	136.73	++	+	6.01	4.11
26$_b$	100.00	131.07	+	+	6.03	1.31
26$_c$	1000.00	139.44	+	+	6.00	-7.17
26$_d$	33.30	30.91	++	++	6.66	-1.08
26$_e$	33.30	45.36	++	++	6.49	1.36

[a] Experimental activity value

[b] Estimated activity value.

[c] Activity scale: 1/C < 10 μM = +++ (highly active); 10 μM ≤ 1/C > 100 μM = ++ (moderately active); 1/C ≥ 100 μM = + (low active).

[d] Fit value calculated by geometry fitting between the hypothesis and the compound; the higher value, the better fit.

[e] Error factor calculated as the ratio of the measured activity to the estimated activity or the inverse if the estimated activity is greater than the measured activity. If measured activity is greater than the estimated activity, the error factor is negative and vice versa.

2.3.2.2. Validation of Hypo 1 pharmacophore model

This step was carried out in order to examine the ability of the developed model to identify active structures and predict their activities precisely. Two methods were applied to validate the hypo 1, test set activity prediction and mapping of glimepiride as an external reference of the generated pharmacophore.

2.3.2.2.1. Test set activity prediction

Test set of seven compounds was prepared using the same protocol as training set, then used to verify the ability of the selected pharmacophore model (hypo 1) to predict the activities of the new chemical compounds. Results demonstrated that hypo 1 is able to predict activities and differentiate between the active and inactive compounds correctly. Values of the experimental and estimated activities of the test set compounds are listed in **Table 5**.

Table 5: Experimental and estimated activities of the test set compounds based on pharmacophore model hypo 1.

Comp.	Exp.[a] (µM)	Est.[b](µM)	Fit value[c]
25_f	20.00	2.30	7.78
25_g	7.14	3.36	7.62
25_h	2.04	5.32	7.42
26_f	NA[d]	128.93	6.03
26_g	NA[d]	134.90	6.02
26_h	NA[d]	134.03	6.02
27	4.00	4.31	7.51

[a] Experimental activity value

[b] Estimated activity value.

[c] Fit value indicates how well the features in the pharmacophore overlap the chemical features in the molecule.

[d] NA: not active

2.3.2.2. 2. Mapping of glimepiride

Mapping of glimepiride as a reported external reference of the generated pharmacophore was demonstrated in **fig. 9**. It was found that the Fit value of glimepiride according to hypo 1 is high (7.51).

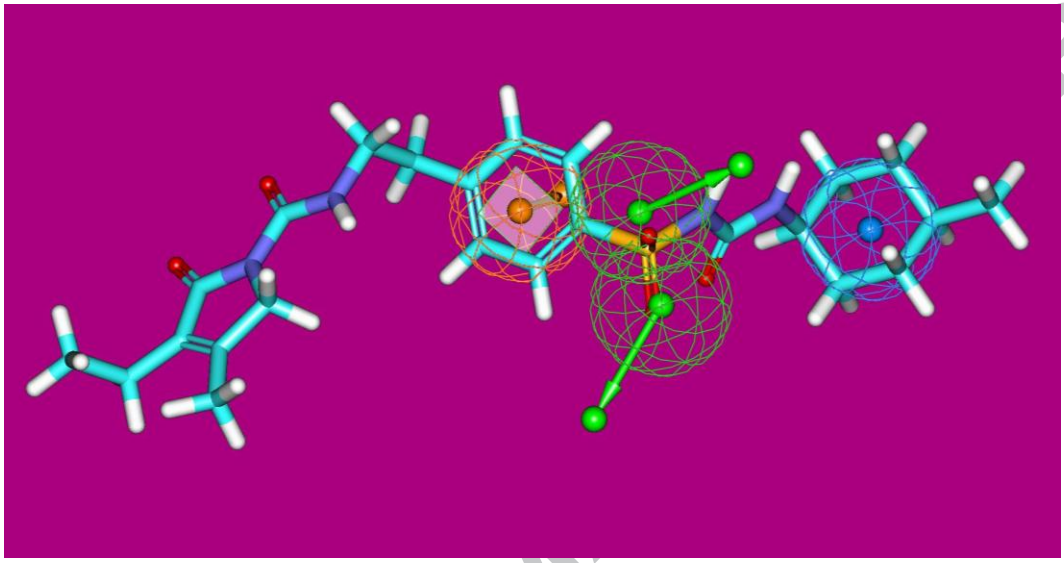

Fig. 9: Mapping of glimepiride on the generated high ranked pharmacophore (Hypo1)

2.3.2.3. Estimation of designed molecules

The valid 3D pharmacophore was used to estimate the activities of the designed molecules to choose the best fitted compounds. The designed molecules were prepared and their activities were estimated according to the fitting with Hypo1. Estimated activities and fit values of the designed compounds were listed in **Table 6**. The result revealed that most of the designed compounds are promising as SUR agonists, and the most promising compounds are arranged in descending order as; **15_b, 19_a, 15_a, 15_d, 19_b, 19_e, 19_d, 24_a** and **15_e**. Mapping of four designed compounds (**15_b**, **15_a**, **19_d**, and **24_a**) on the generated pharmacophore was demonstrated in **Fig. 10, 11, 12** and **13**, respectively.

Table 6: Expected activities and fit values of designed compounds based on the Hypo 1 pharmacophore model

Comp.	Est.[a] (µM)	Fit value[b]	Comp.	Est.[a] (µM)	Fit value[b]
15_a	3.42	7.61	**19_c**	184.34	5.88
15_b	2.55	7.74	**19_d**	7.46	7.28
15_c	126.34	6.05	**19_e**	5.57	7.40
15_d	3.42	7.61	**19_f**	184.70	5.88
15_e	9.92	7.15	**24_a**	7.68	7.26
15_f	102.67	6.14	**24_b**	118.91	6.07
19_a	2.82	7.70	**24_c**	184.58	5.88
19_b	4.84	7.46			

[a] Estimated activity value.

[b] Fit value indicates how well the features in the pharmacophore overlap the chemical features in the molecule.

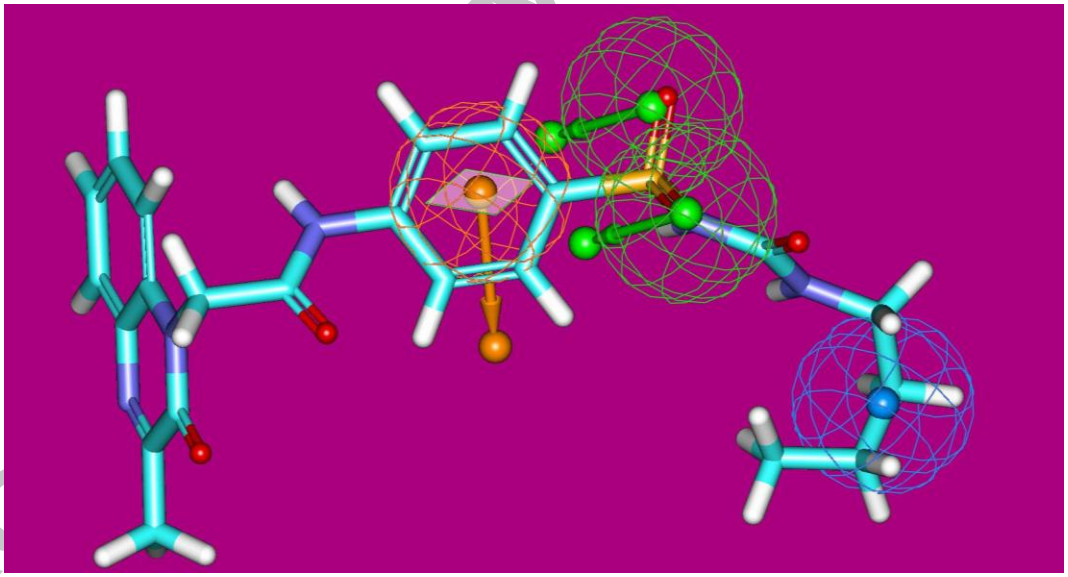

Fig. 10: Mapping of compound **15_b** (fit value = 7.74) on the generated high ranked pharmacophore (Hypo1)

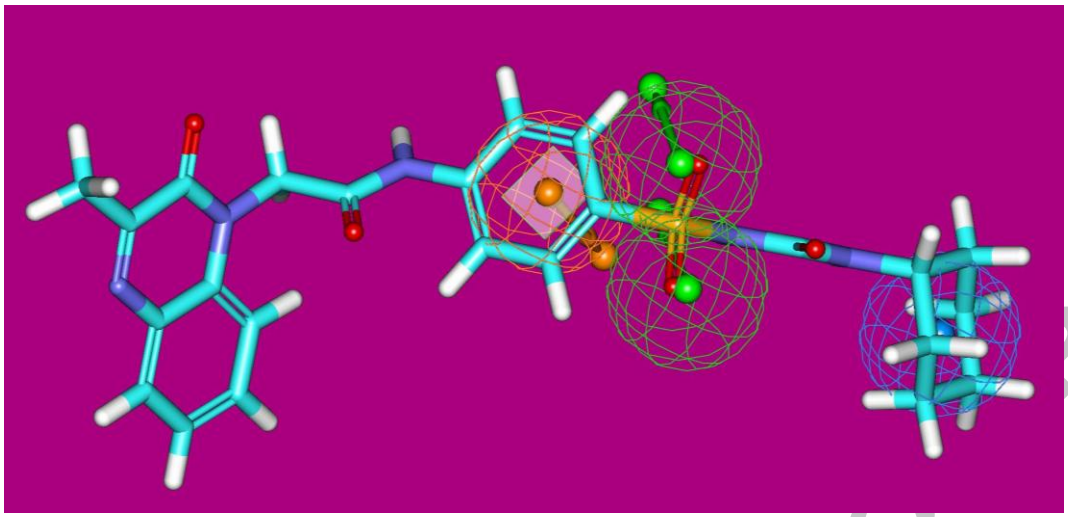

Fig. 11: Mapping of compound **15_a** (fit value = 7.61) on the generated high ranked pharmacophore (Hypo1)

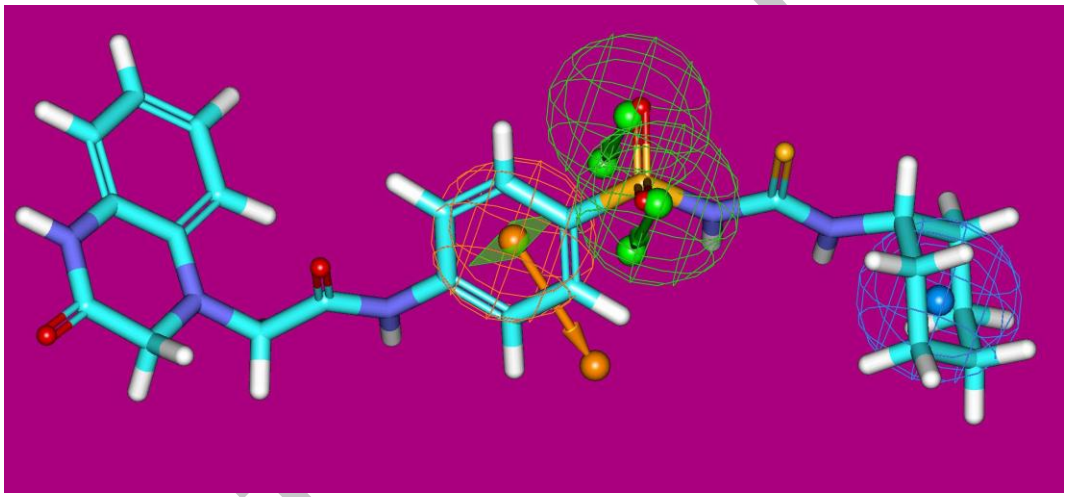

Fig. 12: Mapping of compound **19_d** (fit value = 7.28) on the generated high ranked pharmacophore (Hypo1)

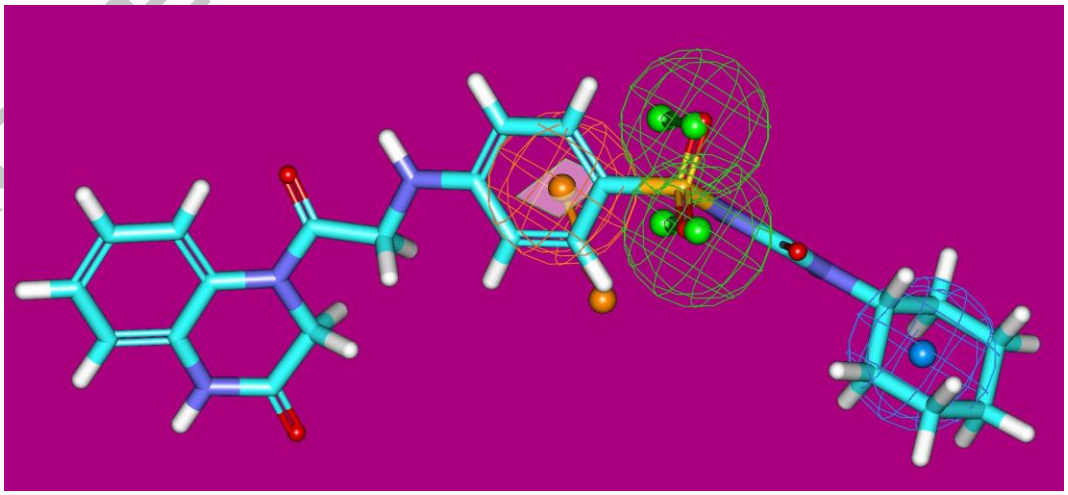

Fig. 13: Mapping of compound **24$_a$** (fit value = 7.26) on the generated high ranked pharmacophore (Hypo1)

2.4. Structure Activity Relationship (SAR)

The newly synthesized compounds were designed to comprise the basic structural requirements of PPARγ and SUR agonists. Observing biological results, we could deduce valuable data about the structure activity relationships.

Firstly, the substitution on the sulfonylurea or sulfonylthiourea moieties was explored. The increased % reduction in blood glucose level values in addition to decreased both IC_{50} and EC_{50} of compounds **15$_a$**, **19$_a$** and **24$_a$**, with incorporated cyclohexyl moiety, than those of their corresponding members **15$_c$**, **19$_c$** and **24$_c$** with incorporated phenyl moiety, indicated that substitution with alicyclic moiety is advantageous. Moreover, substitution of butyl group (open chain aliphatic) resulted in slight decrease of activity comparable to alicyclic substitution, as for compounds **15$_b$**, **19$_b$** and **24$_b$**.

Comparing the anti-hyperglycemic activities of sulfonylurea and sulfonylthiourea derivatives showed that, sulfonylureas were more active than sulfonylthioureas. In addition, sulfonylurea derivatives showed insulin-secreting activities higher than that of sulfonylthioureas. Interestingly, sulfonylthioureas were more active than sulfonylureas as PPARγ binders.

The increased % reduction in blood glucose level values of compounds **15$_{a-f}$**, with incorporated 3-methylquinoxalin-2(1*H*)-one moiety, than those of their corresponding members **19$_{a-f}$** with incorporated 3,4-dihydroquinoxalin-2(1*H*)-one moiety, indicated that substitution with 3-methylquinoxalin-2(1*H*)-one moiety is more preferred biologically.

Finally, the effect of structural modification on the linker between lipophilic tail and an aromatic scaffold (spacer group) has been investigated. Comparing the anti-hyperglycemic activities of compounds **19$_{a-c}$** with that of compounds **24$_{a-c}$**, it was found that changing the position of carbonyl group of the linker did not affect the anti-hyperglycemic activity.

3. Conclusion

In summary, fifteen novel quinoxaline-based derivatives have been designed and synthesized incorporating the substantial sulfonylurea and sulfonylthiourea moieties with the aim of targeting the PPARγ and SURs. The synthesized compounds were evaluated *in-vivo* for their anti-hyperglycemic activities against STZ induced hyperglycemic rats. It was found that many compounds showed good anti-hyperglycemic activities. Two additional *in-vitro* studies were carried out for the most potent anti-hyperglycemic agents to estimate PPARγ binding affinity and insulin-secreting ability as potential mechanisms for anti-hyperglycemic activity. Some of the synthesized compounds (**15_a**, **15_b**, **15_d** and **15_e**) significantly bound to PPARγ with IC_{50} values ranging from 0.350 to 0.491 µM. Moreover, Compounds **15_a** and **15_b** have exhibited potent insulin-secreting activities with EC_{50} values of0.92 and 0.98 µM, respectively. Docking studies was carried out to investigate their binding pattern with the prospective target, PPARγ. Pharmacophore studies were performed to justify the biological activities of the synthesized compounds against SURs. The obtained data from molecular modeling studies showed that most of the synthesized compounds had considerable high affinity towards PPARγ and SURs. The most active candidates may serve as useful lead compounds in search for powerful and selective anti-hyperglycemic agents.

4. Materials and methods

4.1. Chemistry

All melting points were measured on a Gallenkamp melting point apparatus and were uncorrected. The IR spectra were recorded on a Pye-Unicam SP-3-300 infrared spectrophotometer (potassium bromide dicks) and expressed in wave number (cm^{-1}). ^{1}HNMR spectra were run at 400 MHz, on a Varian Mercury VX-300 and Bruker Avance III NMR spectrometer respectively, while ^{13}C NMR spectra were run at 100 MHz. TMS was used as an internal standard in deuterated dimethylsulphoxide (DMSO-*d6*). Chemical shifts (δ) are quoted in ppm. The abbreviations used are as follows: s, singlet; d, doublet; m, multiplet. All coupling constant (*J*) values are given in hertz. The mass spectra were recorded on Shimadzu GCMS-QP-1000EX mass spectrometer at70 eV. Elemental analyses were performed on CHN analyzer and all compounds were within ± 0.4 of the theoretical values. The reactions were monitored by thin-layer chromatography (TLC) using TLC sheets coated with UV fluorescent silica gel Merck 60 F254 plates and were visualized using UV lamp and different solvents as mobile phases. All

reagents and solvents were purified and dried by standard techniques. All the newly synthesized compounds gave satisfactory elemental analysis. Compounds **11, 12, 13, 17, 21** were prepared according to reported methods [31, 32, 34, 35].

4.1.1. 2-(3-Methyl-2-oxoquinoxalin-1(2H)-yl)-N-(4-sulfamoylphenyl) acetamide (14)

A mixture of the potassium salt of 3-methylquinoxalin-2(1*H*)-one **12** (4.00 g, 20.17 mmol), 2-Chloro-*N*-(4-sulfamoylphenyl)acetamide **13** (5.00g, 20.17 mmol) and KI (0.10 g, 0.60 mmol) in DMF (40 ml) was heated on a water bath for 20 h. After cooling, the reaction mixture was poured on crushed ice. The formed precipitate was collected by filtration, dried and washed by boiled absolute ethanol to afford compound **14**.

Yellow powder (yield 76 %, 5.7 g); m.p. 290-293 ^{o}C; IR (KBr, υ cm^{-1}): 3327, 3258 (NH_2), 3118 (C-H aromatic), 1657 (C=O amide), 1601 (C=N quinoxaline), 1534 (amide II band), 1306, 1152 (SO_2); ^{1}H NMR (DMSO-d_6, 400 MHz) δ (ppm): 2.47 (s, 3H, CH_3- quinoxaline), 5.15 (s, 2H, CH_2), 7.24 (s, 2H, D_2O exchangeable, NH_2), 7.33-7.80(m, 4H, Ar-H quinoxaline), 7.51 (d, J = 6.0 Hz, 2H, Ar-H phenyl),7.73 (d, J = 6.0 Hz, 2H, Ar-H phenyl), 10.77 (s, 1H, D_2O exchangeable, NH); ^{13}C NMR (DMSO-d_6, 100MHz) δ(ppm): 21.55 (CH_3), 45.76 (CH_2), 115.14, 119.22, 119.31, 123.91, 127.25, 129.25, 130.14, 132.42, 133.40, 139.16, 141.90, 154.81, 157.92, 165.92; DEPT spectrum differentiated ^{13}C signals to be; one CH_3, one CH_2 and six CH; MS (*m/z*): 372 (M^+, 1.81 %), 202 (11.37 %), 201 (100 %, base peak), 173 (23.89 %), 146 (15.84 %), 145 (72.83), 92 (11.30 %), 77 (14.77 %); Anal. Calcd. for $C_{17}H_{16}N_4O_4S$ (372.40): C, 54.83; H, 4.33, N, 15.05; S: 8.61; Found: C, 55.06; H, 4.37; N, 15.27; S, 8.68.

4.1.2. ***General procedure for synthesis of compounds (15$_{a\text{-}f}$)***

A mixture of of 2-(3-methyl-2-oxoquinoxalin-1(2*H*)-yl)-*N*-(4-sulfamoy lphenyl)acetamide **14** (0.75g, 2.00 mmol) and anhydrous potassium carbonate (0.55 g, 4.00 mmol) in dry acetone (150 ml) was stirred at refluxing temperature for 1.5 h then cooled to room temperature. Next, the appropriate isocyanates or isothiocyanates namely, cyclohexyl isocyanate, butyl isocyanate, phenyl isocyanate, cyclohexyl isothiocyanate, butyl isothiocyanate, and phenyl isothiocyanate (2.20 mmol) was added to the reaction mixture. Refluxing with stirring was continued for 24 h. Acetone was removed by evaporation under reduced pressure, and then water (200 ml) was added to dissolve the resulting residue. The solution was acidified with 1.0 N aqueous

hydrochloric acid (10 ml) and the resulted residue was collected by filtration. Crystallization of the filter cake from 90% aqueous ethanol yielded purified corresponding sulfonyl(thio)urea derivatives **15_{a-f}** respectively.

4.1.2.1. N-{4-[N-(Cyclohexylcarbamoyl)sulfamoyl]phenyl}2-(3-methyl-2-oxoquinoxalin-1(2H)-yl) acetamide (15_a)

White crystals (yield 69.85 %); m.p. 172-175 ˚C; IR (KBr, υ cm^{-1}): 3281, 3205 (3NH, overlapped), 3075 (C-H aromatic), 2932, 2861 (C-H aliphatic), 1676 (C=O amide), 1602 (C=N quinoxaline), 1535 (amide II band) and 1332, 1161 (SO_2);^{1}H NMR (DMSO-d_6, 400 MHz) δ (ppm): 1.03-1.55 (m, 10H, cyclohexyl), 2.47 (s, 3H, CH_3- quinoxaline), 3.42 (m, 1H, CH cyclohexyl), 5.16 (s, 2H, $COCH_2$), 6.33 (d, J = 7.5 Hz, 1H, D_2O exchangeable, NH-cyclohexyl), 7.33 (dd, J = 7.8, 7.2 Hz, 1H, Ar-H- quinoxaline),7.48 (d, J = 7.8 Hz, 1H, Ar-H- quinoxaline), 7.52 (dd, J = 8.1, 7.2 Hz, 1H, Ar-H quinoxaline), 7.77 (d, J = 8.1 Hz, 1H, Ar-H quinoxaline), 7.73 (d, J = 8.7 Hz, 2H, Ar-H phenyl), 7.82 (d, J = 8.7 Hz, 2H, Ar-H phenyl), 10.26 (s, 1H, D_2O exchangeable, SO_2NH), 10.89 (s, 1H, D_2O exchangeable, NH amide);^{13}C NMR (DMSO-d_6, 100 MHz) δ (ppm): 21.55, 24.59, 25.43, 32.70, 45.77, 48.46, 115.11, 119.09, 123.91, 129.08, 129.25, 130.17, 132.42, 133.37, 134.82, 143.08, 150.93, 154.79, 157.92, 166.08; DEPT classified ^{13}C signals into; four CH_2, one CH_3 and seven CH; Anal. Calcd. for $C_{24}H_{27}N_5O_5S$ (497.57): C, 57.93; H, 5.47; N, 14.08; S, 6.44; Found: C, 58.17; H, 5.54; N, 14.26; S, 6.51.

4.1.2.2. N-{4-[N-(Butylcarbamoyl)sulfamoyl]phenyl}2-(3-methyl-2-oxoquinoxalin-1(2H)-yl) acetamide (15_b)

White crystals (yield 68.45 %); m.p. 188-190 ˚C; IR (KBr, υ cm^{-1}): 3274, 3196 (3NH, overlapped), 3105 (C-H aromatic), 2948, 2876 (C-H aliphatic), 1633 (C=O amide), 1601 (C=N quinoxaline), 1535 (amide II band) and 1334, 1160 (SO_2); ^{1}H NMR (DMSO-d_6, 300 MHz) δ (ppm): 0.81 (t, J = 7.5 Hz, 3H, CH_3 butyl), 1.19 (m, 2H, C**H**$_2$$CH_3$), 1.30 (m, 2H, C**H**$_2$$CH_2CH_3$), 2.92 (dt,$J$ = 6.0, 6.3 Hz, 2H, C**H**$_2$$CH_2CH_2CH_3$), 2.48 (s, 3H, CH_3- quinoxaline), 5.16 (s, 2H, $COCH_2$), 6.32 (s, 1H, D_2O exchangeable, NH-butyl),7.33 - 7.77 (m, 4H, Ar-H quinoxaline), 7.71 (d, J = 8.7 Hz, 2H, Ar-H), 7.82 (d, J = 8.7 Hz, 2H, Ar-H), 10.81 (s, 1H, D_2O exchangeable, NH amide).^{13}C NMR (DMSO-d_6, 150 MHz) δ (ppm): 13.97, 18.75, 21.52, 31.75, 39.27, 45.72, 114.96, 119.15, 123.96, 129.00, 129.25, 130.18, 132.40, 133.24, 135.06, 142.98, 152.08, 154.81,

157.93, 166.03; DEPT showed four CH_2, two CH_3 and six CH; Anal. Calcd. for $C_{22}H_{25}N_5O_5S$ (471.53): C, 56.04; H, 5.34; N, 14.85; S, 6.80; Found: C, 56.32; H, 5.37; N, 14.98; S, 6.87.

4.1.2.3. N-{4-[N-(Phenylcarbamoyl)sulfamoyl]phenyl}2-(3-methyl-2-oxoquinoxalin-1(2H)-yl) acetamide (15_c)

White crystals (yield 60.61 %); m.p. 229-231 ˚C; IR (KBr, υ cm^{-1}): 3332 (br, 3NH, overlapped), 3107 (C-H aromatic), 1652 (C=O amide), 1604 (C=N quinoxaline), 1538 (amide II band) and 1327, 1160 (SO_2);^{1}H NMR (DMSO-d_6, 300 MHz) δ (ppm): 2.47 (s, 3H, CH_3- quinoxaline), 5.16 (s, 2H, $COCH_2$), 6.57-7.93 (m, 13H, Ar-H), 7.22 (s, 1H, D_2O exchangeable, NH-phenyl), 8.91 (s, 1H, D_2O exchangeable, SO_2NH), 10.91 (s, 1H, D_2O exchangeable, NH amide).^{13}C NMR (DMSO-d_6, 150 MHz) δ (ppm): 21.54, 45.73, 119.17, 119.33, 123.68, 123.99, 129.24, 129.29, 129.34, 130.24, 132.38, 133.26, 134.45, 138.42, 143.27, 149.84, 154.81, 157.95, 166.09; DEPT revealed one CH_2, one CH_3 and nine CH; Anal. Calcd. for $C_{24}H_{21}N_5O_5S$ (491.52): C, 58.65; H, 4.31; N, 14.25; S, 6.52; Found: C, 58.82; H, 4.29; N, 14.37; S, 6.60.

4.1.2.4. N-{4-[N-(Cyclohexylcarbamothioyl)sulfamoyl]phenyl}2-(3-methyl-2-oxoquinoxalin-1(2H)-yl)acetamide (15_d)

Yellow crystals (yield 62.84 %); m.p. 160-162 ˚C; IR (KBr, υ cm^{-1}): 3484, 3322, 3236 (3NH), 3047 (C-H aromatic), 2931, 2863 (C-H aliphatic), 1670 (CO amide), 1605 (C=N quinoxaline), 1527 (amide II band) and 1316, 1124 (SO_2);^{1}H NMR (DMSO-d_6, 300 MHz) δ (ppm): 1.23-1.88 (m, 10H, cyclohexyl), 2.48 (s, 3H, CH_3- quinoxaline), 3.94 (m, 1H, CH cyclohexyl), 5.17 (s, 2H, $COCH_2$), 7.33-7.77 (m, 4H, Ar-H quinoxaline),7.76-7.86 (m, 4H, Ar-H phenyl), 8.23 (d, J = 6.9 Hz, 1H, D_2O exchangeable, NH-cyclohexyl), 10.93 (s, 1H, D_2O exchangeable, NH amide), 11.26 (s, 1H, D_2O exchangeable, SO_2NH); Anal. Calcd. for $C_{24}H_{27}N_5O_4S_2$ (513.63): C, 56.12; H, 5.30; N, 13.64; S, 12.48; Found: C, 56.31; H, 5.36; N, 13.80; S, 12.56.

4.1.2.5. N-{4-[N-(butylcarbamothioyl)sulfamoyl]phenyl}2-(3-methyl-2-oxoquinoxalin-1(2H)-yl)acetamide (15_e)

Yellow powder (yield 61.10 %); m.p. 140-143 ˚C; IR (KBr, υ cm^{-1}): 3321, 3192 (3NH, overlapped), 3103 (C-H aromatic), 2947 (C-H aliphatic), 1653 (C=O amide), 1597 (C=N quinoxaline), 1535 (amide II band) and 1393, 1158 (SO_2);^{1}H NMR (DMSO-d_6, 400MHz) δ (ppm): 0.80 (t, J = 7.2 Hz, 3H, CH_3 butyl), 1.15 (m, 2H, C**H**$_2$$CH_3$), 1.41 (m, 2H, C**H**$_2$$CH_2CH_3$), 2.46 (s, 3H, CH_3- quinoxaline), 3.39 (dt,2H, C**H**$_2$$CH_2CH_2CH_3$), 5.17 (s, 2H, $COCH_2$), 7.34-7.79 (m, 4H, Ar-H quinoxaline), 7.77 (d, J = 8.4 Hz, 2H, Ar-H phenyl),7.86 (d, J = 8.4 Hz, 2H, Ar-H

phenyl),8.44 (t, J = 5.2 Hz, 1H, D_2O exchangeable, NH-butyl), 10.98 (s, 1H, D_2O exchangeable, NH amide), 11.36 (s, 1H, D_2O exchangeable, SO_2NH);^{13}C NMR (DMSO-d_6, 100 MHz) δ (ppm): 14.03, 19.83, 21.53, 30.17, 44.63, 45.77, 115.02, 119.22, 124.00, 129.20, 129.25, 130.22, 132.39, 133.26, 133.63, 143.47, 154.81, 157.94, 166.14, 178.38; DEPT classified ^{13}C signals to; four CH_2, two CH_3 and six CH; MS (*m/z*): 487 (M^+, 3.59 %), 299 (12.53 %), 285 (5.26 %), 256 (100 %, base peak), 242 (11.42 %), 201 (42.28 %), 199 (12.92 %), 173 (5.44 %), 167 (10.21 %), 156 (40.85 %), 125 (44.66 %), 115 (58.18 %), 92 (44.23 %), 77 (22.37 %), 59 (30.32 %), 44 (52.89 %); Anal. Calcd. for $C_{22}H_{25}N_5O_4S_2$ (487.59): C, 54.19; H, 5.17; N, 14.36; S, 13.15; Found: C, 54.34; H, 5.22; N, 14.51; S, 13.22.

4.1.2.6. N-{4-[N-(phenylcarbamothioyl)sulfamoyl]phenyl}2-(3-methyl-2-oxoquinoxalin-1(2H)-yl)acetamide (15_f)

Yellow crystals (yield 53.8 %); m.p. 209-2011 ˚C; IR (KBr, υ cm^{-1}): 3383, 3200 (3NH, overlapped), 3066 (C-H aromatic), 1664 (C=O amide), 1605 (C=N quinoxaline), 1530 (amide II band) and 1378, 1162 (SO_2); ^{1}H NMR (DMSO-d_6, 400 MHz) δ (ppm): 2.47 (s, 3H, CH_3-quinoxaline), 5.16 (s, 2H, $COCH_2$), 7.00-7.93 (m, 13H, Ar-H), 8.82 (s, 1H, D_2O exchangeable, NH-phenyl),10.66 (s, 1H,D_2O exchangeable, SO_2NH), 10.9 (s, 1H,D_2O exchangeable, NH amide); Anal. Calcd. for $C_{24}H_{21}N_5O_4S_2$ (507.58): C, 56.79; H, 4.17; N, 13.80; S, 12.63; Found: C, 56.96; H, 4.14; N, 14.01; S, 12.72.

4.1.3. 2-(3-Oxo-3,4-dihydroquinoxalin-1(2H)-yl)-N-(4-sulfamoylphenyl)acetamide (18)

A mixture of 3,4-dihydroquinoxalin-2(1*H*)-one **17** (2.98 g, 20.11 mmol), 2-chloro-*N*-(4-sulfamoylphenyl)acetamide **13** (5.00 g, 20.11 mmol), $NaHCO_3$ (1.69 g, 20.11 mmol) and KI (0.10 g, 0.60 mmol, catalytic amount) in DMF (30 ml) was heated on a water bath for 20 h. After cooling, the reaction mixture poured onto crushed ice. The formed precipitate was collected by filtration, dried, washed by boiled absolute ethanol and filtered to give compound **18**.

Yellow powder (yield 72.63); m.p. 250-253 ^{o}C; IR (KBr, υ cm^{-1}): 3382, 3268 (NH_2 & 2NH, overlapped), 3121 (C-H Aromatic), 1668 (C=O amide), 1599 (C=N quinoxaline), 1531 (amide II band), 1307, 1148 (SO_2); ^{1}H NMR (DMSO-d_6, 600 MHz) δ (ppm): 4.02 (s, 2H, $COCH_2$), 4.15 (s, 2H, CH_2 quinoxaline), 7.27 (s, 2H, D_2O exchangeable, NH_2), 6.57 (d, J = 7.8 Hz, 1H, Ar-H quinoxaline), 6.68 (dd, J = 7.8, 7.2 Hz, 1H, Ar-H quinoxaline), 6.83 (d, J = 7.2 Hz, 2H, Ar-H phenyl), 7.77 - 7.80 (m, 4H, Ar-H), 10.44 (s, 1H, D_2O exchangeable, NH amide), 10.50 (s, 1H, D_2O exchangeable, NH quinoxaline); ^{13}C NMR (DMSO-d_6, 150 MHz) δ (ppm): 52.81, 53.59,

111.69, 115.51, 118.97, 119.32, 123.47, 127.19, 127.32, 135.18, 138.91, 142.09, 166.08, 168.92; DEPT spectrum showed two CH_2 and six different CH; MS (*m/z*): 361 (M^++1, 1.33%), 360 (M^+, 7.00%), 281 (15.62 %), 214 (8.65 %), 187 (48.01 %), 172 (80.10 %), 162 (13.30 %), 161 (100 %, base peak), 156 (64.42 %), 147 (30.00 %), 133 (70.70 %), 119 (38.62 %), 92 (76.40 %), 77 (21.77 %), 58 (15.59 %); Anal. Calcd. for $C_{16}H_{16}N_4O_4S$ (360.39): C, 53.32; H, 4.48; N, 15.55; S, 8.90; Found: C, 53.51; H, 4.51; N, 15.78; S, 8.94.

4.1.4. General procedure for synthesis of compounds 19_{a-f}

A mixture of 2-(2-oxo-3,4-dihydroquinoxalin-4(1*H*)-yl)-*N*-(4-sulfamoylphenyl)acetamide **18** (0.72 g, 2 mmol) and anhydrous potassium carbonate (0.55 g, 4 mmol) in dry acetone (150 ml) was stirred at refluxing point for 1.5 h then cooled to room temperature. Next, the appropriate isocyanates or isothiocyanates namely, cyclohexyl isocyanate, butyl isocyanate, phenyl isocyanate, cyclohexyl isothiocyanate, butyl isothiocyanate, and phenyl isothiocyanate (2.20 mmol) was added to the reaction mixture. Refluxing with stirring was continued for 24 h. Acetone was removed by evaporation under reduced pressure, and then water (200 ml) was added to dissolve the resulting residue. The solution was acidified with 1.0 N aqueous hydrochloric acid (10 ml) and the resulted residue was collected by filtration, crystallized 95% aqueous ethanol to yield the corresponding sulfonyl(thio)urea derivatives $\mathbf{19_{a-f}}$, respectively.

4.1.4.1. N-{4-[N-(cyclohexylcarbamoyl)sulfamoyl]phenyl}-2-(3-oxo-3,4-dihydroquinoxalin-1(2H)-yl)acetamide (19_a)

White crystals (yield 63.91 %); m.p. 163-166 ˚C; IR (KBr, υ cm^{-1}): 3278 (br, 4NH, overlapped), 3101 (C-H aromatic), 2930, 2861 (C-H aliphatic), 1683 (C=O amide), 1529 (amide II band) and 1324, 1157 (SO_2); ^{1}H NMR (DMSO-d_6, 400 MHz) δ (ppm): 1.07-1.65 (m, 10H, cyclohexyl), 3.44 (m, 1H, CH cyclohexyl), 3.98 (s, 2H, $COCH_2$) 4.13 (s, 2H, CH_2 quinoxaline), 6.35 (d, J = 6.4 Hz, 1H, D_2O exchangeable, NH-cyclohexyl),6.55-7.86 (m, 8H, Ar-H), 10.26 (s, 1H, D_2O exchangeable, SO_2NH), 10.42 (s, 1H, D_2O exchangeable, NH amide), 10.58 (s, 1H, D_2O exchangeable, NH quinoxaline); MS (*m/z*): 485 (M^+, 2.07 %), 255 (7.15 %), 214 (11.79 %), 190 (2.60 %), 172 (100 %, base peak), 156 (97.11 %), 147 (35.07 %), 133 (63.85 %), 92 (82.66 %), 77 (24.14 %), 58 (17.79 %); Anal. Calcd. for $C_{23}H_{27}N_5O_5S$ (485.56): C, 56.89; H, 5.61; N, 14.42; S, 6.60; Found: C, 57.03; H, 5.68; N, 14.57; S, 6.71.

4.1.4.2. N-{4-[N-(butylcarbamoyl)sulfamoyl]phenyl}-2-(3-oxo-3,4-dihydroquinoxalin-1(2H)-yl)acetamide (19_b).

White crystals (yield 59.91 %); m.p. 180-182 ˚C; IR (KBr, υ cm^{-1}): 3272, (br, 4NH, overlapped), 3103 (C-H aromatic), 2952 (C-H aliphatic), 1682 (C=O amide), 1527 (amide II band) and 1323, 1157 (SO_2); ^{1}H NMR (DMSO-d_6, 400 MHz) δ (ppm): 0.80 (t, J = 7.2 Hz, 3H, CH_3 butyl), 1.17 (m, 2H, C**H**$_2$$CH_3$), 1.28 (m, 2H, C**H**$_2$$CH_2CH_3$), 2.93 (m, 2H, C**H**$_2$$CH_2CH_2CH_3$), 3.98 (s, 2H, $COCH_2$), 4.13 (s, 2H, CH_2 quinoxaline), 6.54 (d, J = 8 Hz, 1H, D_2O exchangeable, NH-butyl), 6.40-7.83 (m, 8H, Ar-H), 10.41 (s, 1H, D_2O exchangeable, NH amide), 10.50 (s, 1H, D_2O exchangeable, SO_2NH),10.55 (s, 1H, D_2O exchangeable, NH quinoxaline); Anal. Calcd. for $C_{21}H_{25}N_5O_5S$ (459.52): C, 54.89; H, 5.48; N, 15.24; S, 6.98 %; Found: C, 55.01; H, 5.54; N, 15.24; S, 7.03.

4.1.4.3. N-{4-[N-(phenylcarbamoyl)sulfamoyl]phenyl}-2-(3-oxo-3,4-dihydroquinoxalin-1(2H)-yl)acetamide (19_c)

White crystals (yield 46.97 %); m.p. 170-172 ˚C; IR (KBr, υ cm^{-1}): 3343 (br, 4NH, overlapped), 3108 (C-H aromatic), 2853 (C-H aliphatic), 1683 (C=O amide), 1532 (amide II band) and 1322, 1157 (SO_2);^{1}H NMR (DMSO-d_6, 400 MHz) δ (ppm): 3.98 (s, 2H, $COCH_2$) 4.12 (s, 2H, CH_2 quinoxaline), 6.52-7.9 (m, 13H, Ar-H), 8.77 (s, 1H, D_2O exchangeable, NH-phenyl), 10.41 (s, 1H, NH amide), 10.55 (s, 1H, D_2O exchangeable, NH quinoxaline), 10.73 (s, 1H, D_2O exchangeable, SO_2NH); Anal. Calcd. for $C_{23}H_{21}N_5O_5S$ (479.51): C: 57.61, H: 4.41, N: 14.61, S: 6.69; Found: C, 57.87; H, 4.38; N, 14.83; S, 6.75.

4.1.4.4. N-{4-[N-(cyclohexylcarbamothioyl)sulfamoyl]phenyl}-2-(3-oxo-3,4-dihydroquinoxalin-1(2H)-yl)acetamide (19_d)

Yellow crystals (yield 59.87 %); m.p.208-211˚C; IR (KBr, υ cm^{-1}): 3323 (br, 4NH, overlapped), 3110 (C-H aromatic), 2932, 2857 (C-H aliphatic), 1680 (C=O amide), 1528 (amide II band) and 1319, 1153 (SO_2). ^{1}H NMR (DMSO-d_6, 400 MHz) δ (ppm): 1.22-1.75 (m, 10H, cyclohexyl), 3.17 (m, 1H, CH cyclohexyl), 3.99 (s, 2H, $COCH_2$), 4.14 (s, 2H, CH_2 quinoxaline), 6.54-7.79 (m, 4H, Ar-H quinoxaline), 7.76-7.83 (m, 4H, Ar-H phenyl), 8.23 (d, J = 7.6 Hz, 1H, D_2O exchangeable, NH-cyclohexyl), 10.42 (s, 1H, D_2O exchangeable, NH amide), 10.63 (s, 1H, D_2O exchangeable, NH quinoxaline), 11.30 (s, 1H, D_2O exchangeable, SO_2NH); Anal. Calcd. for $C_{23}H_{27}N_5O_4S_2$ (501.62): C: 55.07, H: 5.43, N: 13.96, S: 12.78; Found: C, 55.28; H, 5.49; N, 14.13; S, 12.99.

4.1.4.5. N-{4-[N-(butylcarbamothioyl)sulfamoyl]phenyl}-2-(3-oxo-3,4-dihydroquinoxalin-1(2H)-yl)acetamide (19_e)

Yellow crystals (yield 56.83 %); m.p. 185-188 ˚C; IR (KBr, υ cm^{-1}):3327, 3237 (br, 4NH, overlapped), 2961 (C-H aliphatic), 1680 (C=O amide), 1524 (amide II band) and 1316, 1150 (SO_2);^{1}H NMR (DMSO-d_6, 400 MHz) δ (ppm):1.08 (t, 3H, CH_3-butyl), 1.16 (m, 2H, C**H**$_2$$CH_3$), 1.59 (m, 2H, C**H**$_2$$CH_2CH_3$), 3.41 (m, 2H, C**H**$_2$$CH_2CH_2CH_3$), 3.98 (s, 2H, $COCH_2$) 4.13 (s, 2H, CH_2 quinoxaline), 6.30-7.82 (m, 8H, Ar-H), 8.14 (s, 1H, D_2O exchangeable, NH-butyl), 10.42 (s, 1H, D_2O exchangeable, NH amide), 10.56 (s, 1H, D_2O exchangeable, NH quinoxaline), 11.32 (s, 1H, D_2O exchangeable, SO_2NH); Anal. Calcd. for $C_{21}H_{25}N_5O_4S_2$ (475.13): C: 53.04, H: 5.30, N: 14.73, S: 13.48; Found: C, 53.21; H, 5.42; N, 14.82; S, 13.62.

4.1.4.6. N-{4-[N-(phenylcarbamothioyl)sulfamoyl]phenyl}-2-(3-oxo-3,4-dihydroquinoxalin-1(2H)-yl)acetamide (19_f)

Yellow crystals (yield 43.43 %); m.p. 160-163 ˚C; IR (KBr, υ cm^{-1}):3291 (4NH, overlapped), 3068 (C-H aromatic), 1681 (C=O amide), 1522 (amide II band) and 1387, 1153 (SO_2). ^{1}H NMR (DMSO-d_6, 400 MHz) δ (ppm): 3.98 (s, 2H, $COCH_2$) 4.13 (s, 2H, CH_2 quinoxaline), 6.54 - 7.91 (m, 13H, Ar-H), 8.87 (s, 1H, D_2O exchangeable, NH-phenyl), 10.41 (s, 1H, D_2O exchangeable, NH amide), 10.56 (s, 1H, D_2O exchangeable, NH quinoxaline), 10.66 (s, 1H, D_2O exchangeable, SO_2NH); Anal. Calcd. for $C_{23}H_{21}N_5O_4S_2$ (495.57): C: 55.74, H: 4.27, N: 14.13, S: 12.94; Found: C, 55.89; H, 4.29; N, 14.30; S, 13.09.

4.1.5. 4-(2-Oxo-2-(3-oxo-3,4-dihydroquinoxalin-1(2H)-yl)ethylamino)benzenesulfonamide (23)

A mixture of 4-(2-chloroacetyl)-3,4-dihydroquinoxalin-2(1*H*)-one **21** (5.00 g, 22.26 mmol), sulfanilamide **22** (3.83 g, 22.26 mmol), $NaHCO_3$ (1.87 g, 22.26 mmol) and KI (0.10 g, 0.60 mmol) in DMF (50.00 ml) was heated on a water bath for 20 h. After cooling, the reaction mixture was poured onto crushed ice. The resulted precipitate was collected by filtration, dried and crystallized from methanol to give compound **23**.

Yellow powder (yield 62.33 %); m.p. 165-168 ^{o}C; IR (KBr, υ cm^{-1}): 3353, 3234 (NH_2), 3077 (C-H aromatic), 2915 (C-H aliphatic), 1681 (CO amide), 1504 (amide II band) and 1325, 1143 (SO_2); ^{1}H NMR (DMSO-d_6, 600 MHz) δ (ppm): 4.22 (s, 2H, CH_2), 4.40 (s, 2H, CH_2), 6.63 (s, 1H, D_2O exchangeable, NH-phenyl), 6.96 (s, 2H, D_2O exchangeable, NH_2), 6.69 - 7.80 (m, 8H, Ar-H), 10.74 (s, 1H, D_2O exchangeable, NH quinoxaline); ^{13}C NMR (DMSO-d_6, 75 MHz) δ (ppm): 35.79, 44.53, 111.24, 116.39, 122.26, 124.06, 125.96, 127.14, 130.78, 150.97, 162.31,

167.28, 168.90; MS (*m/z*): 360 (M^+, 3.13 %), 188 (11.10 %), 185 (26.10 %), 172 (100 %, base peak), 156 (94.34 %), 146 (78.15 %), 108 (56.01 %), 92 (90.89 %), 77 (9.43 %), 44 (15.62 %); Anal. Calcd. for $C_{16}H_{16}N_4O_4S$ (360.39): C, 53.32; H, 4.48; N, 15.55; S, 8.90; Found: C, 53.47; H, 4.53; N, 15.78; S, 8.98.

4.1.6. General procedure for synthesis of compounds 24_{a-c}

A mixture of 4-(2-oxo-2-(2-oxo-3,4-dihydroquinoxalin-4(1*H*)-yl)ethylamino)benzen sulfonamide **23** (0.72 g, 2.00 mmol) and anhydrous potassium carbonate (0.55 g, 4.00 mmol) in dry acetone (150 ml) was stirred with refluxing for 1.5 h. Then, the reaction mixture was cooled to room temperature. Next, the appropriate isocyanates namely, cyclohexyl isocyanate, butyl isocyanate, and phenyl isocyanate, (2.20 mmol) was added. Refluxing with stirring was continued for 24 h. Acetone was removed by evaporation under reduced pressure, and then water (200 ml) was added to dissolve the resulting residue. The solution was acidified with 1.0 N aqueous hydrochloric acid (10 ml) and the resulted residue was collected by filtration. Upon crystallization of the filter cake from 95% aqueous ethanol, the corresponding sulfonylurea derivatives **24_{a-c},** respectively, were produced.

4.1.6.1. N-(cyclohexylcarbamoyl)-4-(2-oxo-2-(3-oxo-3,4-dihydroquinoxalin-1(2H)-yl)ethyl amino)benzenesulfonamide (24_a)

White crystals (yield 61.85 %); m.p. 167-170 ˚C; IR (KBr, υ cm^{-1}): 3366 (br, 4NH, overlapped), 3087 (C-H aromatic), 2929, 2860 (C-H aliphatic), 1685 (C=O amide), 1525 (amide II band) and 1331, 1150 (SO_2). ^{1}H NMR (DMSO-d_6, 400 MHz) δ (ppm):1.05-1.66 (m, 10H, cyclohexyl), 3.25 (m, 1H, CH cyclohexyl), 4.21 (s, 2H, $COCH_2$) 4.38 (s, 2H, CH_2 quinoxaline), 6.20 (d, J = 8 Hz,1H, D_2O exchangeable, NH-cyclohexyl), 6.77 (s, 1H, D_2O exchangeable, NH-phenyl), 6.62-7.81 (m, 4H, Ar-H quinoxaline), 7.57 (d, J = 9.2 Hz, 2H, Ar-H phenyl),7.68 (d, J = 9.2 Hz, 2H, Ar-H phenyl), 9.95 (s, 1H, D_2O exchangeable, SO_2NH), 10.72 (s, 1H, D_2O exchangeable, NH quinoxaline), Anal. Calcd. for $C_{23}H_{27}N_5O_5S$ (485.56): C, 56.89; H, 5.61; N, 14.42; S, 6.60; Found: C, 57.03; H, 5.72; N, 14.73; S, 6.53.

4.1.6.2. N-(butylcarbamoyl)-4-(2-oxo-2-(3-oxo-3,4-dihydroquinoxalin-1(2H)-yl)ethylamino) benzenesulfonamide (24_b)

White crystals (yield 43.57 %); m.p. 163-166 ˚C; IR (KBr, υ cm^{-1}):3371 (br, 4NH, overlapped), 3102 (C-H aromatic), 2950 (C-H aliphatic), 1685 (C=O amide), 1521 (amide II band) and 1335, 1151 (SO_2). ^{1}H NMR (DMSO-d_6, 400 MHz) δ (ppm): 0.81 (t, J = 7.2 Hz, 3H, CH_3 butyl), 1.16 (m, 2H, C**H**$_2$$CH_3$), 1.27 (m, 2H, C**H**$_2$$CH_2CH_3$), 2.92 (m, 2H, C**H**$_2$$CH_2CH_2CH_3$), 4.21 (s, 2H,

$COCH_2$) 4.38 (s, 2H, CH_2 quinoxaline), 6.31 (s, 1H, D_2O exchangeable, NH-butyl), 6.75 (s, 1H, D_2O exchangeable, NH-phenyl), 6.63-7.68 (m, 4H, Ar-H quinoxaline), 7.53 (d, J = 8.8 Hz, 2H, Ar-H phenyl),7.66 (d, J = 8.8 Hz, 2H, Ar-H phenyl), 10.09 (s, 1H, D_2O exchangeable, SO_2NH), 10.72 (s, 1H, D_2O exchangeable, NH quinoxaline); Anal. Calcd. for $C_{21}H_{25}N_5O_5S$ (459.52): C, 54.89; H, 5.48, N; 15.24, S, 6.98; Found: C, 54.97; H, 5.56; N, 15.39; S, 7.12.

4.1.6.3. N-(phenylcarbamoyl)-4-(2-oxo-2-(3-oxo-3,4-dihydroquinoxalin-1(2H)-yl)ethyl amino) benzenesulfonamide (24_c)

White crystals (yield 52.19 %); m.p.175-178 ˚C; IR (KBr, υ cm^{-1}): 3348 (br, 4NH, overlapped), 3095 (C-H aromatic), 2901 (C-H aliphatic), 1685 (C=O amide), 1520 (amide II band) and 1327, 1149 (SO_2). ^{1}H NMR (DMSO-d_6, 400 MHz) δ (ppm): 4.21 (s, 2H, $COCH_2$) 4.37 (s, 2H, CH_2 quinoxaline), 6.63-7.68 (m, 8H, Ar-H), 7.31 (s, 1H, D_2O exchangeable, NH amine), 8.64 (s, 1H, D_2O exchangeable, CONH-phenyl), 10.46 (s, 1H, D_2O exchangeable, SO_2NH), 10.71 (1H, D_2O exchangeable, NH quinoxaline); Anal. Calcd. for $C_{23}H_{21}N_5O_5S$ (479.51): C, 57.61; H, 4.41; N, 14.61; S, 6.69; Found: C, 57.63; H, 4.42; N, 14.79; S, 6.64.

4.2. Biological testing

4.2.1. In vivo anti-hyperglycemic activity

Anti-hyperglycemic activity screening of the newly synthesized compounds was measured *in vivo* utilizing STZ induced hyperglycemic rats according to reported standard procedure described by Ramsey *et al*. [36] as follows.

The animal experiments were conducted with approval from the Ethics Committee (approval#23PD/3/12/8R) of Al-Azhar University, Nasr City, Cairo, Egypt. All the tests were conducted according to the respective international guidelines. Swiss albino adult male rats, weighing 200 – 300 g, were used as test animals. The rats were housed without any stressful stimuli under well-ventilated conditions at room temperature (25–30 °C). They were allowed to acclimatize with free access to water and food for 24 h period before testing except during the short time they were removed from the cages for testing. Streptozotocin (STZ) (Sigma–Aldrich Chemical Co, Milwaukee, WI, USA) in a dose of 60.00 mg/kg was injected intraperitoneally (i.p.) in 0.90 % sodium citrate buffer (pH 4.50) [42]. After 72 h, the blood sugar level was measured by glucometer. Animals showing blood glucose levels > 250.00 mg/dl were selected for anti-diabetic screening. Diabetic rats were randomly arranged in 18 groups, each of six animals. Fifteen experimental group were administered a suspension of the synthesized

compounds (prepared in 1% gum acacia) orally (20.00 mg/kg body weight). One group served as diabetic control which was also fed with 1% gum acacia. Two groups served as standard control groups, where one received glimepiride (0.36 mg/kg) orally, and the other received rosiglitazone (2.7 mg/kg) orally. Blood samples were collected from the rat tail at 0 and 3 hours after drug administration, blood glucose levels were measured immediately by glucometer. The % reduction in blood glucose level was calculated.

4.2.2. *In vitro* of PPARγ- ligand binding assay

To determine the binding affinity of synthesized compounds to PPARγ, Fluorescence Polarization Assay technique [37] was carried out using Polar Screen^{TM} PPARγ-Competitor Assay Kit (Invitrogen, Carlsbad, CA). According to the manufacturer's instructions, the following procedure was conducted.

Test compounds and the positive control rosiglitazone were dissolved in DMSO with concentration of 0.01–70 µg/ml. The ligand binding domains of PPARγ (LBD) expressed as glutathione *S*-transferase (GST) and Fluormone™ PPARγ green, a tight binding, selective, fluorescent PPARγ ligand, were mixed with test compounds and rosiglitazone.

The PPARγ and Fluormone™ Tracer form a NR/Fluormone™ Tracer complex, resulting in a high polarization value. Compounds that displace the Fluormone™ Tracer from the NR/Fluormone™ Tracer complex cause a decrease in polarization. Displaced Fluormone™ Tracer tumbles rapidly, resulting in a low polarization. The polarization remains high in the presence of compounds which do not displace the Fluormone™ Tracer from the complex. The shift in polarization value in the presence of test compounds is used to determine relative affinity of test compounds for the NR. Displacement of the fluorescent ligand was assessed by measuring loss of fluorescence polarization using a SpectraMax M5 plate reader. From dose repose curve, IC_{50} (Concentration of compound required to displace 50% of titrated ligand) was calculated.

4.2.3. *In vitro* insulin assay

Pancreatic islets of fed Wistar rats (200 - 250 g) injected i.p. with 0.2 ml of a 0.2% pilocarpine solution was isolated by the collagenase method. With this technique, 300 - 400 islets were isolated from each pancreas [43]. The islets were cultured overnight at glucose 16 mmol / l in CMRL-1066 medium containing 2 mmol /l L-glutamine, 10 µg/ml gentamycin, and 10% FCS at 37°C in a 95% air/5% CO_2 atmosphere for 1 h in the presence and the absence of tested compounds dissolved in DMSO (5 uM, 10 uM, 15 uM, 20 uM). Then, the cultured islets were

washed twice in Ringer HEPES buffer and incubated for 30 min at 37°C with glucose 16.7 mmol/ l. Insulin was quantitatively estimated using Rat Insulin ELISA Kit (Thermo Fisher Scientific Inc., USA), according to manufacturer's instructions.

This assay employs the quantitative sandwich enzyme immunoassay technique [38]. Antibody specific for rat insulin (biotinylated anti-rat insulin antibody) has been pre-coated onto a microplate. Standards (recombinant rat insulin, 100 µl) and samples (100 µl) were pipetted into the wells followed by incubation for 2.5 h at room temperature with gentle shaking. Then, Solutions were discarded and the wells were washed 4 times with 1x Wash Solution. After the last wash, the remaining wash buffer was removed by decanting. next, 100 µl of 1x prepared biotinylated antibody was added to each well and incubated for 1 h at room temperature with gentle shaking. Then, washing was performed as before. The prepared Streptavidin-HRP solution (100 µl) was added to each well followed by incubation for 45 min. at room temperature with gentle shaking. The solution was discarded and washed. TMB One-Step Substrate Reagent (100 µl) was added to each well followed by incubation for 30 min. at room temperature in the dark with gentle shaking. Stop Solution (50 µl) was added to each well and the absorbance was read immediately at 450 nm. From a dose response curve, EC_{50} of the compounds were determined.

4.3. Molecular modeling

4.3.1 Docking studies

The 3D crystal structure of the drug target PPARγ was retrieved from RCSB Protein Data Bank [PDB ID- 1FM6, resolution 2.1 Å] (http://www.pdb.org). The docking analysis was performed using Discovery Studio 2.5 software to evaluate the free energies and mode of binding of the designed molecules with the active site of PPARγ. The most promising molecules were selected depending on both correct binding mode and higher binding free energy (ΔG).

The 3D crystal structure of PPARγ receptor (code IFM6) was prepared by removing water molecules and retaining only protein and its crystal ligand. Moreover, the correction of uncorrected valence atoms and crystallographic disorders were performed using alternate conformations and valence monitor options. Then, the 3D protein structure was protonated and its inflexibility was obtained by creating fixed atom constraint. Next, the energy was energy minimized by applying CHARMM (Chemistry at HARvard Macromolecular Mechanics) force fields, and MMFF94 (Merck Molecular force field) force field for charge and partial charge, respectively[44]. The binding site of the protein was defined as receptor molecule and prepared

for docking as follows. The first chain A (protein part) was selected and defined as receptor. Next, the second chain A (ligand part) was selected to define the sphere of 12 Å as binding site.

The 2D structures of ligands (rosiglitazone) and fifteen novel synthesized compounds were sketched using ChemBioDraw Ultra 14.0 and saved in MDL-SD file format. Then, the SD file was opened (by Discovery studio 2.5 software) and 3D structures were protonated. Force fields were applied on the molecules to get lowest energy minimum structures via CHARMM and MMFF94 force fields for charge and partial charge, respectively. Then, each of them was prepared for docking by applying ligand preparation protocol.

The molecular docking of the ligand and tested compounds was performed using CDOCKER protocol which is an implementation of the CDOCKER algorithm [45]. CDOCKER is a grid-based molecular docking method that employs CHARMM-based molecular dynamics (MD) scheme to dock ligands into a receptor binding site [46] . The CDOCKER energy (protein-ligand interaction energy) of best docked poses was calculated and compared with that of rosiglitasone as standard PPARγ agonist.

4.3.2. Pharmacophore studies

A data set consisting 17 compounds possessing a sulfonylurea scaffold **(Fig. 14)** were selected from available literatures (doi: 10.1016/j.bmcl.2009.01.082) [47] and were used in the present study. The selected compounds for the data set shared the same antihyperglycemic assay procedure [47] with wide variations in their structures and potency profiles. The antihyperglycemic activity of SU agonists in the training set span a range of five orders of magnitude or more and reported as µIU/ml for (µIU/ml values range from 20.87 –86.08). Then, the µIU/ml values were converted into the 1/C (the biological activity), where *C* is the concentration of drug required to achieve a defined level of biological activity [48]. Glimepiride was considered as the reference SU agonist.

The 2D structures of ligands were drawn using ChemBioDraw Ultra 14.0, saved in MDL-SD file format, and converted into the corresponding standard 3D structures by Discovery studio 2.5 software. The 3D structures were protonated. Energy minimization process was achieved using CHARMM force field parameter [49]. The resulting structures were then used for the pharmacophore studies.

The Catalyst HypoGen algorithm in Discovery Studios (DS) 2.5 [50] was used to generate 3D pharmacophore models for the SUR agonistic activities. The ligands were divided into a training set (10 compounds) and a testing set (7 compounds) to establish and validate the

3D pharmacophore model. During the process, a maximum of 255 different conformers was generated for each ligand using the best flexible conformation generation module, which performs a precise energy minimization in both torsion and Cartesian space to attain the best coverage of the conformational space [51, 52].

Uncertainty in the activity value was set as 1.5 instead of the default value 3. Minimum interfeature distance was set to be 1.5. Conformation generation was set to be fast. The chosen features to be considered in pharmacophore generation were hydrogen bond donor (HBD), hydrogen bond acceptor (HBA), negative ionizable, hydrophobic aliphatic (HA) and aromatic ring (RA).

The quality of the generated pharmacophore models was validated by two important calculated cost values: fixed cost and null cost. A significant pharmacophore model should have the value of the total cost close to the fixed cost and very different from the null cost, while the configuration value that enumerates the entropy of the hypothetical space should be less than 17 [53, 54]. Moreover, the descriptors of the root mean square (RMS) and the correlation coefficient for the training and testing sets were used to evaluate and select the pharmacophore model. Based on these criteria, virtual screening was carried out via the ligand pharmacophore mapping protocol. The best predictive model was used as 3D queries to identify potential leads against SUR from the newly synthesized compounds.

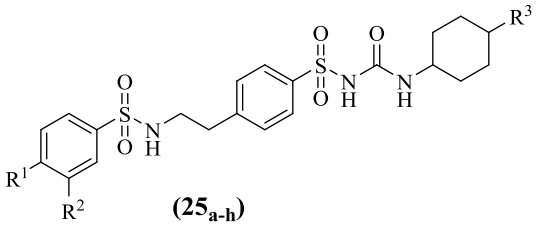

(25_{a-h})

Comp.	a[a]	b[a]	c[a]	d[a]	e[a]	f[b]	g[b]	h[b]
R^1 =	Br	H	H	Cl	Br	$NHCOCH_3$	$NHCOCH_3$	Cl
R^2 =	H	H	H	H	H	H	CH_3	H
R^3 =	CH_3	H	CH_3	H	H	CH_3	CH_3	CH_3

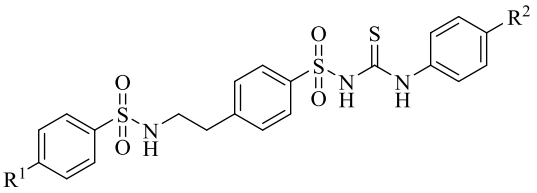

(26_{a-h})

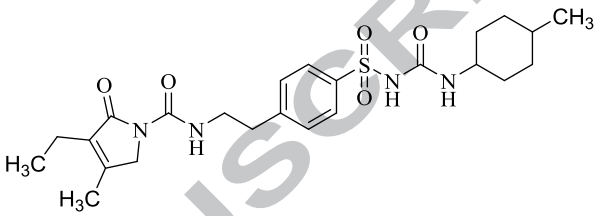

Glimepiride(**27**)

Comp.	a[a]	b[a]	c[a]	d[a]	e [a]	f[b]	g[b]	h[b]
R^1 =	H	H	H	Cl	Cl	CH_3	CH_3	CH_3
R^2 =	Cl	CH_3	OCH_3	Cl	OCH_3	Cl	CH_3	OCH_3

[a] Training set: Conpounds $\mathbf{25_{a-e}}$, $\mathbf{26_{a-e}}$

[b] Test set: Conpounds $\mathbf{25_{f-h}}$, $\mathbf{26_{f-h}}$, **27**

Fig. 14: Chemical structures of training set and test set molecules**.**

Conflict of Interest:

None

Acknowledgement

Authors are thankful to prof. Ahmed Mansour and his scientific team of pharmacology department, faculty of pharmacy, Al-Azhar University, Cairo, Egypt, as well as the biologists of VACSERA CO., Giza, Egypt for providing laboratory facilities for biological testing.

Appendix A. Supplementary data

Supplementary data related to this manuscript is found in separated file.

References

[1] R. Kumar, A. Mittal, U. Ramachandran, Design and synthesis of 6-methyl-2-oxo-1, 2, 3, 4-tetrahydro-pyrimidine-5-carboxylic acid derivatives as PPARγ activators, Bioorganic & medicinal chemistry letters, 17 (2007) 4613-4618.

[2] B. Gross, B. Staels, PPAR agonists: multimodal drugs for the treatment of type-2 diabetes, Best Practice & Research Clinical Endocrinology & Metabolism, 21 (2007) 687-710.

[3] J.M. Lehmann, L.B. Moore, T.A. Smith-Oliver, W.O. Wilkison, T.M. Willson, S.A. Kliewer, An antidiabetic thiazolidinedione is a high affinity ligand for peroxisome proliferator-activated receptor γ (PPARγ), Journal of Biological Chemistry, 270 (1995) 12953-12956.

[4] U. Panten, M. Schwanstecher, C. Schwanstecher, Sulfonylurea receptors and mechanism of sulfonylurea action, Experimental and clinical endocrinology & diabetes, 104 (1996) 1-9.

[5] A. Schmidt, N. Endo, S.J. Rutledge, R. Vogel, D. Shinar, G.A. Rodan, Identification of a new member of the steroid hormone receptor superfamily that is activated by a peroxisome proliferator and fatty acids, Molecular Endocrinology, 6 (1992) 1634-1641.

[6] S. Tyagi, P. Gupta, A.S. Saini, C. Kaushal, S. Sharma, The peroxisome proliferator-activated receptor: A family of nuclear receptors role in various diseases, Journal of advanced pharmaceutical technology & research, 2 (2011) 236.

[7] D.P. Marciano, M.R. Chang, C.A. Corzo, D. Goswami, V.Q. Lam, B.D. Pascal, P.R. Griffin, The therapeutic potential of nuclear receptor modulators for treatment of metabolic disorders: PPARγ, RORs, and Rev-erbs, Cell metabolism, 19 (2014) 193-208.

[8] N. Mahindroo, C.-F. Huang, Y.-H. Peng, C.-C. Wang, C.-C. Liao, T.-W. Lien, S.K. Chittimalla, W.-J. Huang, C.-H. Chai, E. Prakash, Novel indole-based peroxisome proliferator-activated receptor agonists: design, SAR, structural biology, and biological activities, Journal of medicinal chemistry, 48 (2005) 8194-8208.

[9] S. Khanna, R. Bahal, P.V. Bharatam, In silico Studies on PPARγ Agonistic Heterocyclic Systems, QSAR and Molecular Modeling Studies in Heterocyclic Drugs I, Springer2006, pp. 149-180.

[10] T.M. Willson, M.H. Lambert, S.A. Kliewer, Peroxisome proliferator-activated receptor γ and metabolic disease, Annual review of biochemistry, 70 (2001) 341-367.

[11] B.Y. Kim, J.B. Ahn, H.W. Lee, S.K. Kang, J.H. Lee, J.S. Shin, S.K. Ahn, C.I. Hong, S.S. Yoon, Synthesis and biological activity of novel substituted pyridines and purines containing 2, 4-thiazolidinedione, European journal of medicinal chemistry, 39 (2004) 433-447.

[12] T.M. Willson, J.E. Cobb, D.J. Cowan, R.W. Wiethe, I.D. Correa, S.R. Prakash, K.D. Beck, L.B. Moore, S.A. Kliewer, J.M. Lehmann, The structure-activity relationship between peroxisome proliferator-activated receptor γ agonism and the antihyperglycemic activity of thiazolidinediones, Journal of medicinal chemistry, 39 (1996) 665-668.

[13] B.R. Henke, S.G. Blanchard, M.F. Brackeen, K.K. Brown, J.E. Cobb, J.L. Collins, W.W. Harrington, M.A. Hashim, E.A. Hull-Ryde, I. Kaldor, N-(2-benzoylphenyl)-L-tyrosine PPARγ agonists. 1. Discovery of a novel series of potent antihyperglycemic and antihyperlipidemic agents, Journal of medicinal chemistry, 41 (1998) 5020-5036.

[14] M. Oguchi, K. Wada, H. Honma, A. Tanaka, T. Kaneko, S. Sakakibara, J. Ohsumi, N. Serizawa, T. Fujiwara, H. Horikoshi, Molecular design, synthesis, and hypoglycemic activity of a series of thiazolidine-2, 4-diones, Journal of medicinal chemistry, 43 (2000) 3052-3066.

[15] B.R. Henke, 1. Peroxisome proliferator-activated receptor gamma (PPARgamma) ligands and their therapeutic utility, Progress in medicinal chemistry, 42 (2003) 1-53.

[16] K.A. Reddy, B. Lohray, V. Bhushan, A.S. Reddy, N.R. Mamidi, P.P. Reddy, V. Saibaba, N.J. Reddy, A. Suryaprakash, P. Misra, Novel antidiabetic and hypolipidemic agents. 5. Hydroxyl versus benzyloxy containing chroman derivatives, Journal of medicinal chemistry, 42 (1999) 3265-3278.

[17] A. Zask, I. Jirkovsky, J.W. Nowicki, M.L. McCaleb, Synthesis and antihyperglycemic activity of novel 5-(naphthalenylsulfonyl)-2, 4-thiazolidinediones, Journal of medicinal chemistry, 33 (1990) 1418-1423.

[18] R.L. Dow, B.M. Bechle, T.T. Chou, D.A. Clark, B. Hulin, R.W. Stevenson, Benzyloxazolidine-2, 4-diones as potent hypoglycemic agents, Journal of medicinal chemistry, 34 (1991) 1538-1544.

[19] S.W. Goldstein, R.E. McDermott, E.M. Gibbs, R.W. Stevenson, Hydroxyurea derivatives as hypoglycemic agents, Journal of medicinal chemistry, 36 (1993) 2238-2240.

[20] H. Shinkai, S. Onogi, M. Tanaka, T. Shibata, M. Iwao, K. Wakitani, I. Uchida, Isoxazolidine-3, 5-dione and noncyclic 1, 3-dicarbonyl compounds as hypoglycemic agents, Journal of medicinal chemistry, 41 (1998) 1927-1933.

[21] R.M. Lago, P.P. Singh, R.W. Nesto, Congestive heart failure and cardiovascular death in patients with prediabetes and type 2 diabetes given thiazolidinediones: a meta-analysis of randomised clinical trials, The Lancet, 370 (2007) 1129-1136.

[22] S.E. Nissen, K. Wolski, Effect of rosiglitazone on the risk of myocardial infarction and death from cardiovascular causes, New England Journal of Medicine, 356 (2007) 2457-2471.

[23] K.J. Herbst, C. Coltharp, L.M. Amzel, J. Zhang, Direct activation of Epac by sulfonylurea is isoform selective, Chemistry & biology, 18 (2011) 243-251.

[24] W.H. Vila-Carriles, G. Zhao, J. Bryan, Defining a binding pocket for sulfonylureas in ATP-sensitive potassium channels, The FASEB Journal, 21 (2007) 18-25.

[25] S. Fukuen, M. Iwaki, A. Yasui, M. Makishima, M. Matsuda, I. Shimomura, Sulfonylurea agents exhibit peroxisome proliferator-activated receptor γ agonistic activity, Journal of Biological Chemistry, 280 (2005) 23653-23659.

[26] K. Inukai, M. Watanabe, Y. Nakashima, N. Takata, A. Isoyama, T. Sawa, S. Kurihara, T. Awata, S. Katayama, Glimepiride enhances intrinsic peroxisome proliferator-activated receptor-γ activity in 3T3-L1 adipocytes, Biochemical and biophysical research communications, 328 (2005) 484-490.

[27] A. Arrault, S. Rocchi, F. Picard, P. Maurois, B. Pirotte, J. Vamecq, A short series of antidiabetic sulfonylureas exhibit multiple ligand PPARγ-binding patterns, Biomedicine & Pharmacotherapy, 63 (2009) 56-62.

[28] V. Zoete, A. Grosdidier, O. Michielin, Peroxisome proliferator-activated receptor structures: ligand specificity, molecular switch and interactions with regulators, Biochimica et Biophysica Acta (BBA)-Molecular and Cell Biology of Lipids, 1771 (2007) 915-925.

[29] A. Pharmacodynamics, Clinical Pharmacology of Sulfonylureas, Oral antidiabetics, (1996) 199.

[30] V.A. Dixit, P.V. Bharatam, SAR and computer-aided drug design approaches in the discovery of peroxisome proliferator-activated receptor γ activators: A perspective, Journal of Computational Medicine, 2013 (2013).

[31] M. Ali, M. Ismail, M. El-Gaby, M. Zahran, Y. Ammar, Synthesis and antimicrobial activities of some novel quinoxalinone derivatives, Molecules, 5 (2000) 864-873.

[32] M.-K. Ibrahim, A.A. Abd-Elrahman, R.R. Ayyad, K. El-Adl, A.M. Mansour, I.H. Eissa, Design and synthesis of some novel 2-(3-methyl-2-oxoquinoxalin-1 (2H)-yl)-N-(4-(substituted) phenyl) acetamide derivatives for biological evaluation as anticonvulsant agents, Bulletin of Faculty of Pharmacy, Cairo University, 51 (2013) 101-111.

[33] M. Weil, 2-Chloro-N-(4-sulfamoylphenyl) acetamide, Acta Crystallographica Section E: Structure Reports Online, (2005).

[34] Y.R. Bonuga, A.R. Nathb, B. Balramc, B. Ramc, Synthesis and antibacterial activity of 3, 4-dihydroquinoxalin-2 (1H)-one derivatives.

[35] W.A. Bayoumi, S.H. Abdel-Rhman, M.E. Shaker, Synthesis and Evaluation of New 2-Iminothiazolidin-4-one and Thia-zolidin-2, 4-dione Derivatives as Antimicrobial and Anti-inflammatory Agents.

[36] D.J. Ramsey, H. Ripps, H. Qian, Streptozotocin-induced diabetes modulates GABA receptor activity of rat retinal neurons, Experimental eye research, 85 (2007) 413-422.

[37] D.M. Jameson, G. Mocz, Fluorescence polarization/anisotropy approaches to study protein-ligand interactions, Protein-ligand interactions: methods and applications, (2005) 301-322.

[38] S.D. Schmidt, M.J. Mazzella, R.A. Nixon, P.M. Mathews, Aβ measurement by enzyme-linked immunosorbent assay, Amyloid Proteins: Methods and Protocols, (2012) 507-527.

[39] T. Lengauer, M. Rarey, Computational methods for biomolecular docking, Current opinion in structural biology, 6 (1996) 402-406.

[40] Q. Gao, L. Yang, Y. Zhu, Pharmacophore based drug design approach as a practical process in drug discovery, Current computer-aided drug design, 6 (2010) 37-49.

[41] R. Kroemer, Molecular modelling probes: docking and scoring, BioChemical Society Transactions, 31 (2003) 980-984.

[42] Y. Tanko, M. Yerima, M. Mahdi, A. Yaro, K. Musa, A. Mohammed, Hypoglycemic activity of methanolic stem bark of adansonnia digitata extract on blood glucose levels of streptozocin-induced diabetic wistar rats, International Journal of Applied Research in Natural Products, 1 (2008) 32-36.

[43] F. Purrello, M. Vetri, C. Gatta, D. Gullo, R. Vigneri, Effects of high glucose on insulin secretion by isolated rat islets and purified β-cells and possible role of glycosylation, Diabetes, 38 (1989) 1417-1422.

[44] B. Roux, Y. Won, G. Archontis, C. Bartels, S. Boresch, A. Caisch, L. Caves, Q. Cui, A. Dinner, M. Feig, CHARMM: the biomolecular simulation program, J Comput Chem, 30 (2009) 1545614Capriotti.

[45] D.-D. Li, F. Fang, J.-R. Li, Q.-R. Du, J. Sun, H.-B. Gong, H.-L. Zhu, Discovery of 6-substituted 4-anilinoquinazolines with dioxygenated rings as novel EGFR tyrosine kinase inhibitors, Bioorganic & medicinal chemistry letters, 22 (2012) 5870-5875.

[46] J. Sun, D.-D. Li, J.-R. Li, F. Fang, Q.-R. Du, Y. Qian, H.-L. Zhu, Design, synthesis, biological evaluation, and molecular modeling study of 4-alkoxyquinazoline derivatives as potential VEGFR2 kinase inhibitors, Organic & biomolecular chemistry, 11 (2013) 7676-7686.

[47] H.-b. Zhang, Y.-a. Zhang, G.-z. Wu, J.-p. Zhou, W.-l. Huang, X.-w. Hu, Synthesis and biological evaluation of sulfonylurea and thiourea derivatives substituted with benzenesulfonamide groups as potential hypoglycemic agents, Bioorganic & medicinal chemistry letters, 19 (2009) 1740-1744.

[48] G.L. Patrick, An introduction to medicinal chemistry, Oxford university press2013.

[49] B.R. Brooks, R.E. Bruccoleri, B.D. Olafson, D.J. States, S. Swaminathan, M. Karplus, CHARMM: A program for macromolecular energy, minimization, and dynamics calculations, Journal of computational chemistry, 4 (1983) 187-217.

[50] D.S. Version, 2.5 (DS 2.5) User Manual; Accelrys Inc, San Diego, CA, USA, 34 (2009).

[51] I.-J. Chen, N. Foloppe, Conformational sampling of druglike molecules with MOE and catalyst: implications for pharmacophore modeling and virtual screening, Journal of chemical information and modeling, 48 (2008) 1773-1791.

[52] A. Mittal, S. Paliwal, M. Sharma, A. Singh, S. Sharma, D. Yadav, Pharmacophore based virtual screening, molecular docking and biological evaluation to identify novel PDE5 inhibitors with vasodilatory activity, Bioorganic & medicinal chemistry letters, 24 (2014) 3137-3141.

[53] M. Arooj, S. Thangapandian, S. John, S. Hwang, J.K. Park, K.W. Lee, 3D QSAR pharmacophore modeling, in silico screening, and density functional theory (DFT) approaches for identification of human chymase inhibitors, International journal of molecular sciences, 12 (2011) 9236-9264.

[54] R.S. Nayana, S.K. Bommisetty, K. Singh, S.K. Bairy, S. Nunna, A. Pramod, R. Muttineni, Structural analysis of carboline derivatives as inhibitors of MAPKAP K2 using 3D QSAR and docking studies, Journal of chemical information and modeling, 49 (2009) 53-67.

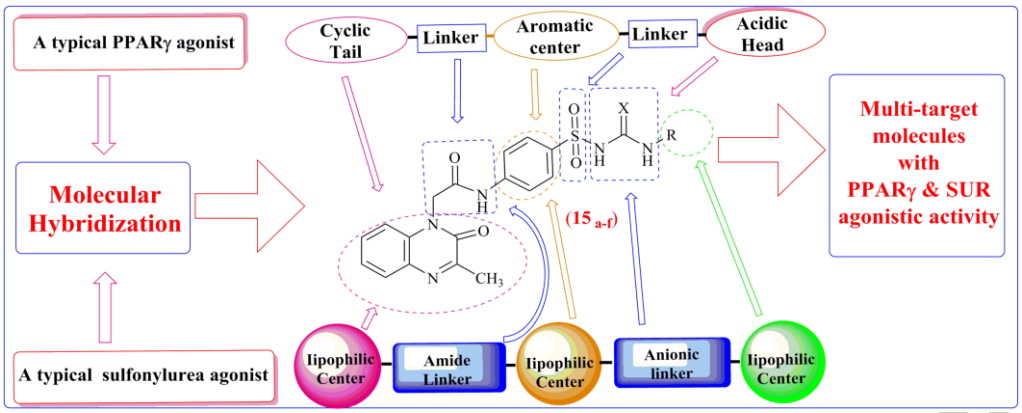

Highlights

- Eighteen compounds of novel quinoxaline derivatives were designed and synthesized.
- Molecular docking and pharmacophore studies were carried out.
- *In vivo* anti-hyperglycemic activity, *in vitro* PPARγ binding affinity and insulin-secreting ability were carried out.
- Some of the synthesized compounds showed promising anti-hyperglycemic activity.